

Contents in this file

1. Responses to the referees' comments
2. Author's changes in the manuscript
3. A marked-up manuscript version showing the changes

Response to Reviewer #1

We are grateful to the reviewer for the thoughtful comments on the manuscript. Our point-to-point responses to each comment are as follows (reviewer's comments are in black font and our responses are in blue font).

General Comments

In this manuscript the authors report a combined experimental and modelling study of the formation and fate of acylperoxy radicals formed from the reaction of α -pinene with ozone in a flow reactor. The alkyl and acyl RO₂ radicals and highly oxidized molecules (HOMs) were monitored using a chemical ionization mass spectrometer with nitrate ion ionization. RO₂ radicals and HOMs were assigned based on elemental formulas and acyl RO₂ radicals were distinguished from alkyl RO₂ radicals by addition of NO₂, which forms RC(O)OONO₂ (acyl peroxy nitrates) that are relatively stable under the conditions of the experiments, thus removing acyl RO₂ signal. Because the changes in acyl RO₂ concentrations can also impact other aspects of the chemistry, a detailed FOAM model employing a modified Master Chemical Mechanism was employed to interpret the results.

Overall, the experiments and modelling were well done and the approach seems to have yielded quite useful and interesting results. The authors provide a very thorough and thoughtful discussion of the results, which is clearly written and easy to follow. Considering the high technical quality of the study and the importance of these reactions to the formation of HOMs and ROOR dimers, both of which are currently of much interest because of their potential role in secondary organic aerosol (SOA) formation, I think the paper is well suited for ACP. I have only a few minor comments.

Specific Comments

1. Line 137: I don't understand the point of converting signals to "concentrations" using sulfuric acid since the actual concentrations will be highly sensitive to the structure of the RO₂ radical and HOM. Presenting the results this way is misleading. Since the "concentrations" are only used to calculate contributions of various species relative to each other, normalized signals will give the same results and be a more honest presentation of the data.

Response: Thanks for the reviewer's comment. We have changed the normalized concentrations of various species to their normalized signals in the revised manuscript.

2. Line 149: Have the authors considered partitioning of RO₂ radicals to particles and what influence that could have on the results? The vapor pressures of the radicals should be similar to those of HOMs, so I don't see any reason that they would not form SOA, and they likely undergo different reactions in the particles since isomerization would be restricted.

Response: We appreciate the reviewer's point. We used a scanning mobility particle sizer (SMPS, TSI) employing both long and nano differential mobility analyzers (model 3081 and 3085 for different particle sizes) to clarify whether there is SOA formation in the experiments. We did not observe SOA formation by SMPS in Exps 1-28. Only in Exp 31 where the reacted α -pinene reaches 36.8 ppb, we observed SOA formation with very low particle mass concentrations (5.0×10^{-4} - 5.7×10^{-3} $\mu\text{g m}^{-3}$) and number concentrations (63-395 # cm^{-3}). Therefore, we suggest that the negligible to low formation of SOA under these experimental conditions has no significant influence on the RO₂ fates.

We have added the results to Section 2.1 of the revised manuscript.

"To clarify whether there is SOA formation in the experiments, a scanning mobility particle sizer (SMPS, TSI), which consists of an electrostatic classifier (model 3080), a long or nano differential mobility analyzer (model 3081 and 3085 for different particle sizes), and a condensation particle counter (model 3087), was used to monitor the formation of SOA particles. Except in Exp 31 where the reacted α -pinene reached 36.8 ppb and there was low SOA formation with particle mass concentrations of 5.0×10^{-4} - 5.7×10^{-3} $\mu\text{g m}^{-3}$ and number concentrations of 63-395 # cm^{-3} , no particle formation was observed by SMPS. Therefore, the RO₂ radicals and closed-shell products would be primarily distributed in the gas phase, with their fates negligibly influenced by the low SOA formation under these experimental conditions."

3. Line 342: In this section it is not clear to me what conclusions are based on measurements, modelling, or a combination of the two. Please make that more clear.

Response: To be more precise, we have clarified the relevant descriptions using "measured signals" and

“simulated contributions” in this section.

4. Line 530: Considering that $\text{RO}_2 + \text{NO}_2$ rate constants have been measured for a variety of alkyl and acyl RO_2 radicals and are pretty consistently $\sim 1\text{E}-11$ (Orlando & Tyndall 2012), it seems unlikely that the value is as low as suggested here. Any explanation based on RO_2 structure would imply that the same effects apply to the $\text{RO}_2 + \text{NO}$ rate constant, which is essentially identical to the NO_2 value (Orlando & Tyndall 2012). This would have significant consequences for predictions of conditions under which autoxidation reactions are important in the atmosphere, since this usually depends on the competition between RO_2 isomerization and the $\text{RO}_2 + \text{NO}$ reaction. What are other possible explanations for the apparent discrepancy?

Response: We appreciate the reviewer’s point. Orlando and Tyndall (2012) have summarized that the rate coefficients of functionalized $\text{RO}_2 + \text{NO}_2$ are in the range of $(5-10)\times 10^{-12} \text{ cm}^3 \text{ molecule}^{-1} \text{ s}^{-1}$. However, these coefficients are mainly for the RO_2 species with small molecular sizes. A recent study by Berndt et al. (2015) determined a $\text{RO}_2 + \text{NO}_2$ rate coefficient of $(1.6\pm 0.5)\times 10^{-12} \text{ cm}^3 \text{ molecule}^{-1} \text{ s}^{-1}$ for a highly oxidized acyl RO_2 radical $\text{O}_2\text{C}-\text{C}_6\text{H}_7(\text{OOH})_2\text{O}_2$ arising from the gas-phase ozonolysis of cycloalkanes, which is several times smaller the rates reported for the relatively simple RO_2 (Orlando and Tyndall, 2012). Therefore, it is possible that some of the α -pinene-derived RO_2 radicals react with NO_2 less efficiently than the smaller RO_2 radicals do. Such differences in the $\text{RO}_2 + \text{NO}_2$ rate coefficient may partially explain the observed increase in $\text{C}_{20}\text{H}_{34}\text{O}_x$ dimer formation as a function of added NO_2 .

References:

- Berndt, T., Richters, S., Kaethner, R., Voigtländer, J., Stratmann, F., Sipilä, M., Kulmala, M., and Herrmann, H.: Gas-Phase Ozonolysis of Cycloalkenes: Formation of Highly Oxidized RO_2 Radicals and Their Reactions with NO , NO_2 , SO_2 , and Other RO_2 Radicals, *J. Phys. Chem. A*, 119, 10336-10348, 10.1021/acs.jpca.5b07295, 2015.
- Orlando, J. J. and Tyndall, G. S.: Laboratory studies of organic peroxy radical chemistry: an overview with emphasis on recent issues of atmospheric significance, *Chem. Soc. Rev.*, 41, 6294-6317, <https://doi.org/10.1039/C2CS35166H>, 2012.

Response to Reviewer #2

We are grateful to the reviewer for the thoughtful comments on the manuscript. Our point-to-point responses to each comment are as follows (reviewer's comments are in black font and our responses are in blue font).

General Comments

In this study, the authors investigated the fraction of acyl peroxy radicals (RO_2) formed from α -pinene ozonolysis. Acyl- RO_2 s are of crucial atmospheric importance due to their higher reactivity and their role in the formation of aerosol precursors. In flow reactor α -pinene ozonolysis experiments, NO_2 was used as an acyl- RO_2 scavenger, and the reduction in RO_2 signals was used to probe the fraction of acyl- RO_2 s produced. The paper is well written and makes a significant contribution towards the better understanding of a key aerosol forming system in the atmosphere. I recommend the publication of the manuscript in ACP after the authors address my minor comments below:

In addition to dimer formation and producing RO, alkyl- RO_2 cross reactions also lead to $\text{ROH} + \text{R}=\text{O}$ products, and if the initial peroxy radical group is on a primary carbon atom, the $\text{R}=\text{O}$ can be a source of acyl- RO_2 following a secondary OH reaction. Alkyl RO_2 s can have significant yields for this reaction. Was this accounted for in the model and in the analysis of the experiments?

Response: Thanks for the reviewer's comment. During the OH oxidation of α -pinene, acyl RO_2 can be formed from the secondary OH oxidation of aldehydes such as pinonaldehyde. However, in the present study, the secondary OH oxidation is significantly inhibited due to an excess of α -pinene compared to O_3 , therefore the contribution of secondary OH oxidation to acyl RO_2 formation is expected to be relatively small. We considered the secondary OH oxidation in the model simulations, and found that the contribution of secondary OH oxidation to acyl RO_2 formation is negligible even under the high O_3 condition (Exp 22, 500 ppb α -pinene + 180 ppb O_3). As shown in Figure S9, the acyl RO_2 $\text{C}_9\text{H}_{13}\text{O}_4$ (C_89CO_3 in Figure S9a) and $\text{C}_{10}\text{H}_{15}\text{O}_5$ (C_920CO_3 in Figure S9b) can be formed from both C-C cleavage/H-shift of $\text{C}_{10}\text{H}_{15}\text{O}_4\text{-RO}$ (Figure 4) and OH oxidation of the first-generation aldehyde products. However, the contributions from secondary OH oxidation are negligible for the two acyl RO_2 species during the whole reaction period under the high O_3 condition (Exp 22, 500 ppb α -pinene + 180 ppb O_3). In addition, the acyl RO_2 $\text{C}_{10}\text{H}_{15}\text{O}_4$ (C_96CO_3) that can be only formed from OH oxidation of pinonaldehyde contributes to only 0.01% and 0.2% of the total $\text{C}_{10}\text{H}_{15}\text{O}_4\text{-RO}_2$ and total acyl RO_2 concentration, respectively. Therefore, the contribution of secondary OH oxidation to acyl RO_2 in this study is minor and the majority of acyl RO_2 species measured here are formed from the ozonolysis channel.

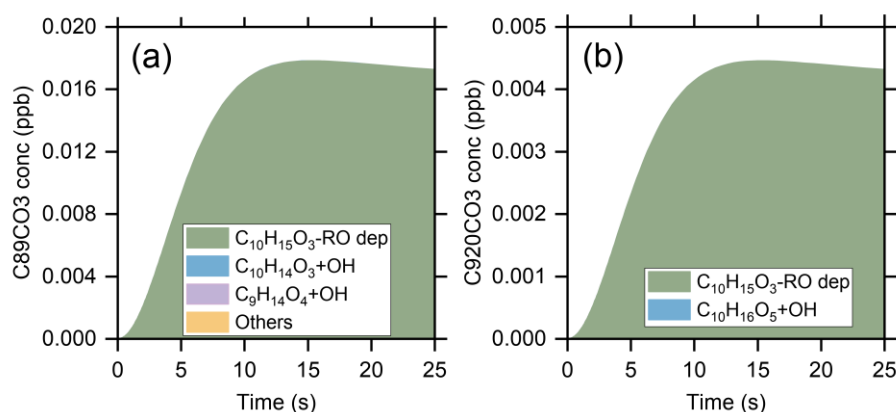


Figure S9 Simulated contribution of different processes to the formation of (a) $\text{C}_9\text{H}_{13}\text{O}_4$ (C_89CO_3) and (b) $\text{C}_{10}\text{H}_{15}\text{O}_5$ (C_920CO_3) acyl- RO_2 during ozonolysis of α -pinene (Exp 22, 500 ppb α -pinene + 180 ppb O_3).

We have added the following discussions to Section 3.2 of the main text.

“In addition, the secondary OH oxidation of aldehyde products can also produce acyl RO_2 radicals during ozonolysis of α -pinene. However, in the present study, the secondary OH oxidation is expected to be

insignificant due to an excess of α -pinene compared to O_3 . Indeed, kinetic model simulations incorporating the secondary OH chemistry show that the contribution of secondary OH oxidation to acyl RO_2 formation is negligible even under high O_3 conditions (see details in Section S2 and Figure S9)”

We have also added the following content and Figure S10 to the SI.

“S2. Contribution of secondary OH oxidation to acyl RO_2 formation.

Considering that the secondary OH oxidation of aldehyde products can also contribute to the formation of acyl RO_2 during ozonolysis of α -pinene, kinetic model simulations incorporating secondary OH chemistry were also performed under typical experimental conditions. As shown in Figure S9, the acyl RO_2 $C_9H_{13}O_4$ (C89CO3 in Figure S9a,) and $C_{10}H_{15}O_5$ (C920CO3 in Figure S9b) can be formed from both C-C cleavage/H-shift of $C_{10}H_{15}O_4$ -RO (Figure 4) and OH oxidation of the first-generation aldehyde products. However, the contributions from secondary OH oxidation are negligible for the two acyl RO_2 species during the whole reaction period. In addition, the acyl RO_2 $C_{10}H_{15}O_4$ (C96CO3) that can be only formed from OH oxidation of pinonaldehyde contributes to only 0.01% and 0.2% of the total $C_{10}H_{15}O_4$ - RO_2 and total acyl RO_2 concentration, respectively (not shown). Therefore, the contribution of secondary OH oxidation to acyl RO_2 in this study is minor and the majority of acyl RO_2 species measured here are formed from the ozonolysis channel.”

The more functionalized acyl- RO_2 s with an -OOH group elsewhere in the molecule are known to undergo H-scrambling reactions to form peroxy acids (R-C(O)OOH) at rates of $1E3 - 1E5$ s⁻¹ (Knap et al. 2017, J. Phys. Chem. A, 121(7), pp.1470-1479). Can the authors comment on the possible role of this reaction in their experiments? For example, the ring-opened acyl $C_{10}H_{15}O_8$ - RO_2 that they report has a 1,6 H-scramble available that leads to a peroxy acid and an alkyl RO_2 . For their model system, Knap et al. estimate a rate coefficient for the 1,6 H-shift of $1.5E5$ s⁻¹. If the rate coefficient is comparable for the alpha-pinene derived $C_{10}H_{15}O_8$ acyl- RO_2 above, this could to an extent explain the low reduction in signal upon NO_2 addition.

Response: We appreciate the reviewer’s point. We have performed a model simulation to evaluate the influence of H-scrambling reactions on the response of ring-opened acyl $C_{10}H_{15}O_8$ - RO_2 to NO_2 addition. As shown in Figure S14, when a 1,6 H-shift rate of 1×10^5 s⁻¹ is considered, the extent of the reduction in $C_{10}H_{15}O_8$ - RO_2 with NO_2 addition indeed becomes smaller, especially when the yield of ring-opened $C_{10}H_{15}O_4$ - RO_2 in the model is at a higher limit (89%). Therefore, the H-scrambling reactions of the ring-opened acyl $C_{10}H_{15}O_8$ - RO_2 could to certain extent explain the low reduction in its signal upon NO_2 addition.

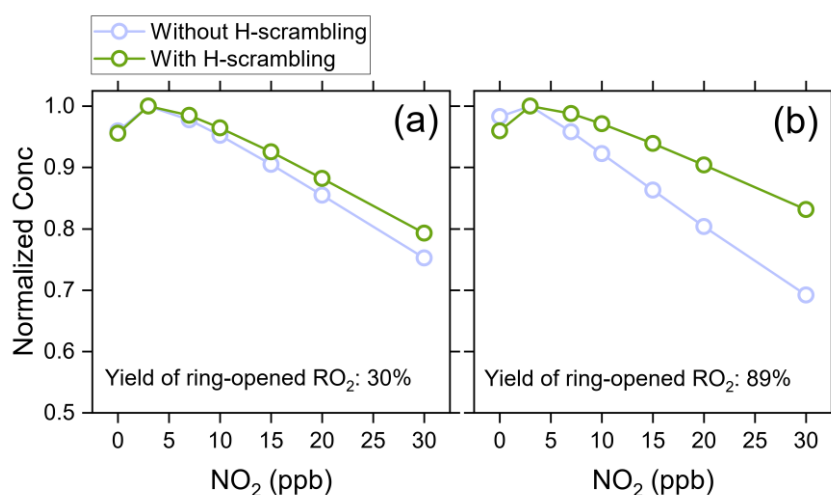


Figure S14 Simulated influence of H-scrambling reaction on the behavior of the ring-opened acyl $C_{10}H_{15}O_8$ - RO_2 as a function of added NO_2 concentration (Exps 8-14). A 1,6 H-scrambling rate of 1×10^5 s⁻¹ and an alkyl RO_2 + NO_2 rate coefficient of 5×10^{-12} cm³ molecule⁻¹ s⁻¹ were used in the model.

We have added the following discussions to Section 3.3 in the main text.

“Thirdly, the ring-opened $C_{10}H_{15}O_8$ - RO_2 , a highly functionalized acyl RO_2 radical with an -OOH group, may be able to undergo very fast intramolecular H-scrambling reactions to form a peroxy acid as

suggested by Knap and Jørgensen (2017), which would compete with the NO₂ reaction and result in a lower reduction in its signal upon NO₂ addition (see details in Section S3)”

We have also added the following content and Figure S14 to the SI.

“S3 Possible influence of H-scrambling reactions on the behavior of C₁₀H₁₅O₈ acyl-RO₂

It has been suggested that the functionalized acyl RO₂ radicals with an -OOH group could undergo H-scrambling reactions to form peroxy acids at rates of 1×10³-1×10⁵ s⁻¹ (Knap and Jørgensen, 2017). Here, we performed a model simulation to evaluate the influence of this reaction on the response of the ring-opened acyl C₁₀H₁₅O₈-RO₂ to NO₂ addition. As shown in Figure S14, considering a 1,6 H-shift rate of 1×10⁵ s⁻¹, the simulated reduction in total C₁₀H₁₅O₈-RO₂ concentration with the addition of 30 ppb NO₂ decreases from 25% to 21% for a C₁₀H₁₅O₄-RO₂ yield of 30% (lower limit) and from 31% to 17% for a yield of 89% (higher limit). These results suggest that the H-scrambling reactions of the ring-opened acyl C₁₀H₁₅O₈-RO₂ could to certain extent explain the low reduction in its signal upon NO₂ addition.”

Line 468: Regarding the speculation of the formation of alkyl C₉H₁₅O₃-RO₂ to explain the discrepancy between experiments and simulations, this would compete with the formation of the ring-opened and ring-retaining C₁₀H₁₅O₄-RO₂. How did the sensitivity analysis of including the C₉H₁₅O₃-RO₂ in the model affect the yield of the C₁₀H₁₅O₄-RO₂s and the subsequent acyl-RO₂s derived from them?

Response: We have evaluated the influence of the sensitivity analysis of C₉H₁₅O₃-RO₂ yield on other C₁₀H₁₅O₄-RO₂ as well as on the contribution of acyl RO₂ to total C₇₋₁₀ HOMs. As shown in Figure S16, as the C₉H₁₅O₃-RO₂ yield increases from 0% to 3%, the simulated concentration of a ring-retaining C₁₀H₁₅O₄-RO₂ radical (C10H15O4KB) decreases by only ~5% and other C₁₀H₁₅O₄-RO₂ species are basically unchanged. As the C₉H₁₅O₃-RO₂ is considered to only produce highly oxygenated alkyl RO₂ in the model, the increase in its yield results in a decrease in the contribution of acyl RO₂ to the total C₉ HOMs. However, the contributions of acyl RO₂ to total C₇, C₈, and C₁₀ HOMs are almost unchanged. These results indicate that the relatively small production of C₉H₁₅O₃-RO₂ has no significant influence on the yield of C₁₀H₁₅O₄-RO₂ and the subsequent acyl RO₂.

We have added the above results and discussion to Section 3.3 in the main text and Figure S16 to the SI.

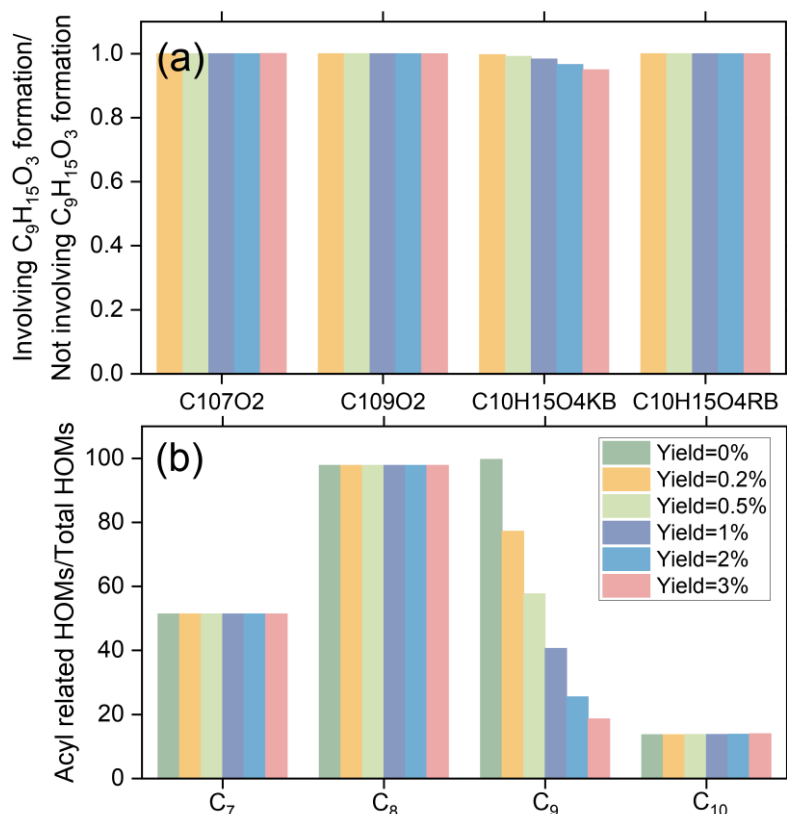


Figure S16 Influences of C₉H₁₅O₃-RO₂ production on (a) the yield of C₁₀H₁₅O₄-RO₂ and (b) the

contribution of acyl RO₂ to total C₇₋₁₀ HOMs (Taking Exp 8 as an example). The C₁₀H₁₅O₄KB and C₁₀H₁₅O₄RB denote a ring-retaining and a ring-opened C₁₀H₁₅O₄-RO₂, respectively (see Table S3 and the main text).

Are any of the acyl peroxy nitrates detected by the NO₃-CIMS? Alpha-pinene derived APNs with 8 oxygen atoms or more should have at least 2 -OOH functional groups and will presumably cluster well with NO₃. Do the decrease in e.g. C₇ and C₈ RO₂ signals when NO₂ is added show an increase in the corresponding APN signals? I think a spectrum figure maybe in the supplementary showing the acyl-RO₂ and acyl-ROONO₂ peaks would be useful.

Response: We have added a spectrum figure in SI showing the signal changes of acyl RO₂ and their corresponding RC(O)OONO₂ (Figure S3). It can be seen that the signals of acyl RO₂ decrease remarkably with the addition of NO₂. Accordingly, the signals of highly oxygenated RC(O)OONO₂ such as C₉H₁₃O₉NO₂, C₉H₁₇O₇NO₂, and C₁₀H₁₅O₇NO₂ increase significantly. We note that some of RC(O)OONO₂ have very similar m/z values with some alkyl RO₂. For example, the m/z values of C₈H₁₃O₆NO₂ (251.0641) and C₈H₁₃O₈NO₂ (283.0539) are very close to those of C₉H₁₅O₈-RO₂ (251.0767) and C₉H₁₅O₁₀-RO₂ (283.0665), respectively, which always have high ion signals. As a result, although some RC(O)OONO₂ are expected to be formed with NO₂ addition, they could not be unambiguously detected by nitrate-CIMS due to their overlapping with strong alkyl RO₂ peaks in this study.

We have added the following discussions to Section 3.1 in the main text.

“Along with the marked reduction in acyl RO₂ signals, the production of highly oxygenated RC(O)OONO₂ species such as C₉H₁₃O₉NO₂, C₉H₁₇O₇NO₂, and C₁₀H₁₅O₇NO₂ with the addition of NO₂ were observed (see the spectra in Figure S3). However, we note that although some RC(O)OONO₂ such as C₈H₁₃O₆NO₂ and C₈H₁₃O₈NO₂ are expected to be formed with NO₂ addition, they could not be unambiguously detected by nitrate-CIMS due to the overlapping of their peaks with strong alkyl RO₂ peaks (C₉H₁₅O₈-RO₂ and C₉H₁₅O₁₀-RO₂) in this study.”

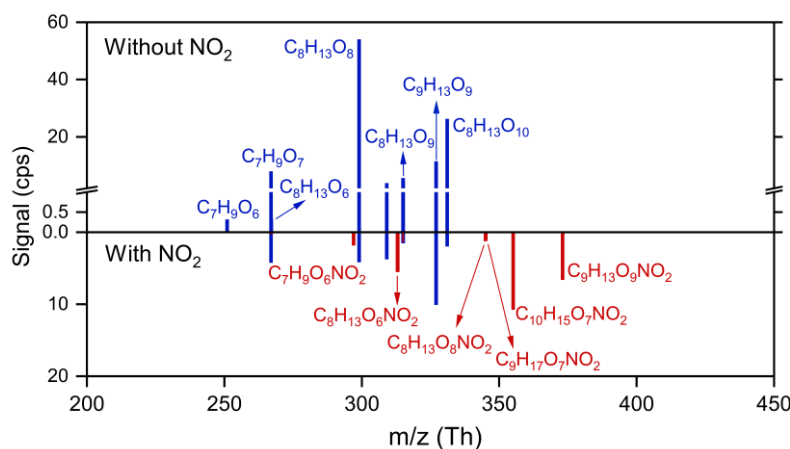
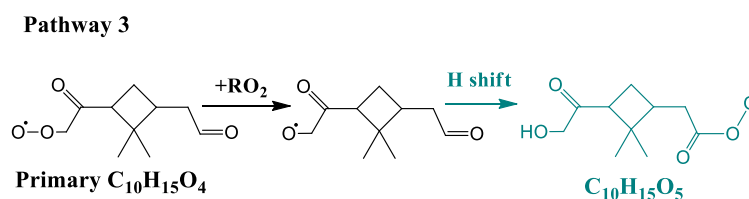


Figure S3 Signals of measured acyl RO₂ and the related RC(O)OONO₂ with and without the addition of NO₂ (Exps 8 and 14).

Figure 4. In pathway 3, the final H-shift of the acyl-oxy is unlikely to compete with CO₂ See reaction r12 and description therein in Vereecken et al. 2009, Phys. Chem. Chem. Phys. 11(40), pp.9062-9074.

Response: Thanks for the reviewer's comment. We have updated pathway 3 with a C₁₀H₁₅O₃ alkoxy radical that can undergo H-shift to form an acyl RO₂.



References:

Knap, H. C. and Jørgensen, S.: Rapid Hydrogen Shift Reactions in Acyl Peroxy Radicals, *J. Phys. Chem. A*, 121, 1470-1479, 10.1021/acs.jpca.6b12787, 2017.

Author's changes in the manuscript

Major changes made in the manuscript are as follows:

Title: We have modified the manuscript title "Acylperoxy radicals during ozonolysis of α -pinene: composition, formation mechanism, and contribution to the production of highly oxygenated organic molecules" to "Direct probing of acylperoxy radicals during ozonolysis of α -pinene: constraints on radical chemistry and production of highly oxygenated organic molecules". We think the new title better highlights the novelty of the study and sounds more attractive.

Line 139-147: We have added a paragraph summarizing the results of SMPS measurements of potential particle formation in the flow tube experiments as well as its potential influence on the fate of organic peroxy radicals and closed-shell products in the gas phase.

Line 244-250: We have provided a mass spectrum showing the formation of acylperoxy nitrates from the reaction of acyl RO₂ with NO₂ in Figure S3 and summarized the results in the main text.

Line 305-309: We have included an evaluation on the contribution of secondary OH oxidation of aldehyde products to the formation of acyl RO₂ species during ozonolysis of α -pinene. More details about the evaluation are provided in Section S2 of the SI.

Line 464-468: We have added an analysis of the possible influence of H-scrambling reactions on the behavior of C₁₀H₁₅O₈ acyl-RO₂. More details about this analysis are provided in Section S3 of the SI.

Line 497-502: We have added a discussion regarding the influence of the production of C₉H₁₅O₃-RO₂ from α -pinene-derived Criegee intermediates on the yield of C₁₀H₁₅O₄-RO₂ and the subsequent acyl RO₂.

Throughout the manuscript: We have changed the normalized concentrations of various species to their normalized signals in the revised manuscript according to the reviewer's suggestion.

Other changes can be found in the marked-up manuscript version enclosed here.

1 **Direct probing of Acylperoxy radicals during ozonolysis of α -pinene: composition,**
2 **formation mechanism, and contribution to constraints on radical chemistry and the**
3 **production of highly oxygenated organic molecules**

4 Han Zang¹, Dandan Huang², Jiali Zhong³, Ziyue Li¹, Chenxi Li¹, Huayun Xiao¹, Yue Zhao^{1,*}

5

6 ¹School of Environmental Science and Engineering, Shanghai Jiao Tong University, Shanghai,
7 200240, China

8 ²Shanghai Academy of Environmental Sciences, Shanghai 200233, China

9 ³Division of Environment and Sustainability, Hong Kong University of Science and Technology,
10 Hong Kong SAR, 999077, China

11

12 *Correspondence: Yue Zhao (yuezhao20@sjtu.edu.cn)

13

14 **Abstract**

15 Acylperoxy radicals (RO₂) are key intermediates in atmospheric oxidation of organic compounds
16 and different from the general alkyl RO₂ radicals in reactivity. However, direct probing of the
17 molecular identities and chemistry of acyl RO₂ remains quite limited. Here, we report a combined
18 experimental and kinetic modelling study of the composition and formation mechanisms of acyl
19 RO₂, as well as their contributions to the formation of highly oxygenated organic molecules (HOMs)
20 during ozonolysis of α -pinene. We find that acyl RO₂ radicals account for 67%, 94%, and 32% of
21 the highly oxygenated C₇, C₈, and C₉ RO₂, respectively, but only a few percent of C₁₀ RO₂. The
22 formation pathway of acyl RO₂ species depends on their oxygenation level. The highly oxygenated
23 acyl RO₂ (oxygen atom number ≥ 6) are mainly formed by the intramolecular aldehydic H-shift (i.e.,
24 autoxidation) of RO₂, while the less oxygenated acyl RO₂ (oxygen atom number < 6) are basically
25 derived from the C-C bond cleavage of alkoxy (RO) radicals containing an α -ketone group or the
26 intramolecular H-shift of RO containing an aldehyde group. The acyl RO₂-involved reactions
27 explain 50-90% of C₇ and C₈ closed-shell HOMs and 14% of C₁₀ HOMs, respectively. For C₉ HOMs,
28 this contribution can be up to 30%-60%. In addition, acyl RO₂ contribute to 50%-95% of C₁₄-C₁₈
29 HOM dimer formation. Because of the generally fast reaction kinetics of acyl RO₂, the acyl RO₂ +
30 alkyl RO₂ reactions seem to outcompete the alkyl RO₂ + alkyl RO₂ pathways, thereby affecting the
31 fate of alkyl RO₂ and HOM formation. Our study sheds lights on the detailed formation pathways
32 of the monoterpene-derived acyl RO₂ and their contributions to HOM formation, which will help to
33 understand the oxidation chemistry of monoterpenes and sources of low-volatility organic
34 compounds capable of driving particle formation and growth in the atmosphere.

35 1. Introduction

36 Monoterpenes ($C_{10}H_{16}$) comprise an important fraction of nonmethane hydrocarbons in the global
37 atmosphere (Guenther et al. 2012, Sindelarova et al. 2014) and make a significant contribution to
38 the secondary organic aerosol (SOA) budget (Pye et al. 2010, Iyer et al. 2021). The presence of
39 double bond and large molecular size of monoterpenes favor their oxidation reactivity towards O_3 ,
40 hydroxyl (OH), and nitrate (NO_3) radicals (Berndt 2022, Roger et al. 2004, Atkinson, Hasegawa
41 and Aschmann 1990, Kurten et al. 2015, Kristensen et al. 2016, Bianchi et al. 2019), as well as the
42 formation of low-volatility products and SOA (Molteni et al. 2019, Shen et al. 2022, Bianchi et al.
43 2019, Zhang et al. 2018, Fry et al. 2014, Fry et al. 2009). The organic peroxy radicals (RO_2) in the
44 gas-phase oxidation of monoterpenes can undergo autoxidation and form a class of highly
45 oxygenated organic compounds (HOM) (Bianchi et al. 2019, Jokinen et al. 2014, Mentel et al. 2015,
46 Berndt et al. 2016, Berndt 2022, Zhao, Thornton and Pye 2018, Bell et al. 2021), which are primarily
47 low- or extremely low-volatility organic compounds (LVOCs and ELVOCs) (Bianchi et al. 2019,
48 Ehn et al. 2014) and thus play a crucial role in SOA formation and growth.

49 Significant advances have been made in recent years concerning the monoterpene RO_2 autoxidation
50 and its contribution to HOM formation (Zhao et al. 2018, Shen et al. 2022, Ehn et al. 2014, Berndt
51 et al. 2016, Xu et al. 2019, Berndt 2022, Lin et al. 2021). It is recognized that a part of monoterpene
52 RO_2 radicals derived from the traditional ozonolysis channel (i.e., isomerization of Criegee
53 intermediates, CI) and OH addition channel can autoxidize at a rate larger than 1 s^{-1} and could be
54 an important contributor to HOM formation (Zhao et al. 2018, Xu et al. 2019, Berndt 2021).
55 Recently, new reaction channels leading to the RO_2 radicals that can undergo fast autoxidation have
56 been proposed. A quantum chemical calculation study indicated that an excited CI arising from α -
57 pinene ozonolysis could undergo ring-breaking reactions and directly lead to a ring-opened RO_2 due
58 to the excess energy, which can autoxidize at a rate of $\sim 1\text{ s}^{-1}$ and rapidly form highly oxidized RO_2
59 with up to 8 oxygen atoms (Iyer et al. 2021). In addition, the minor hydrogen abstraction channel
60 by OH radicals has been proposed as a predominant pathway to HOM formation from OH oxidation
61 of α -pinene under atmospheric conditions (Shen et al. 2022).

62 RO_2 species can be simply divided into alkyl RO_2 and acyl RO_2 ($RC(O)OO$) according to whether
63 R is an acyl radical. There are significant differences in the reactivity of these two kinds of RO_2 .
64 Firstly, the rate constant of acyl RO_2 with NO is in general slightly higher than that of alkyl RO_2
65 (Orlando and Tyndall 2012, Calvert et al. 2008, Atkinson et al. 2007). For example, the reaction
66 rate constants of acyl RO_2 , $CH_3C(O)O_2$, and alkyl RO_2 , $CH_3CH_2O_2$, with NO have been reported to
67 be $20 \times 10^{-12}\text{ cm}^3\text{ molecule}^{-1}\text{ s}^{-1}$ and $9.2 \times 10^{-12}\text{ cm}^3\text{ molecule}^{-1}\text{ s}^{-1}$, respectively (Orlando and Tyndall

68 2012, Calvert et al. 2008, Atkinson et al. 2007). Besides, acyl RO₂ can react rapidly with NO₂ and
69 form thermally unstable peroxyacyl nitrates (RC(O)OONO₂), which have a lifetime of tens of
70 minutes at room temperature and of days and even months in winter or in the upper atmosphere with
71 lower temperatures (Orlando and Tyndall 2012, Atkinson et al. 2007). Although alkyl RO₂ radicals
72 can also react with NO₂ and form the alkyl peroxy nitrates (ROONO₂), they are extremely unstable
73 and will decompose into RO₂ radicals and NO₂ in less than 1s (Orlando and Tyndall 2012, Kirchner
74 et al. 1997). Lastly, the rate constant of cross-reaction of acyl RO₂ ($1.5 \pm 0.3 \times 10^{-11} \text{ cm}^3 \text{ molecule}^{-1} \text{ s}^{-1}$)
75 is significantly higher than that of alkyl RO₂ ($2 \times 10^{-17} - 1 \times 10^{-11} \text{ cm}^3 \text{ molecule}^{-1} \text{ s}^{-1}$) (Zhao et
76 al. 2018, Tyndall et al. 2001, Atkinson et al. 2007, Villenave and Lesclaux 1996). As a result, these
77 two kinds of RO₂ may play different roles in the autoxidation as well as HOM and dimer formation.

78 The quantum calculations revealed that different functional groups in RO₂ would lead to
79 significantly different intramolecular H-shift rates (Otkjær et al. 2018). The C=O and C=C
80 substituents lead to resonance stabilized carbon radicals and could enhance the H-shift rate constants
81 by more than a factor of 400. The fast aldehydic H-shift rate contributes to a series of acyl radicals
82 (RC(O)) with the radical site at the terminal carbonyl carbon, which further produce the acyl RO₂
83 with O₂ addition. Many RO₂ formed in the oxidation of monoterpenes have the aldehyde
84 functionality, especially for α -pinene ozonolysis, in which all the primary and many later-generation
85 RO₂ contain at least one aldehyde group (Berndt et al. 2018, Berndt 2022, Li et al. 2019, Noziere et
86 al. 2015, Shen et al. 2022). As a result, acyl RO₂ may comprise a considerable fraction of total RO₂
87 species and contribute significantly to the formation of low-volatility products and SOA in the
88 monoterpene oxidation system. A recent study by Zhao et al. (2022) found that the acyl RO₂-
89 involved reactions contribute to 50%-80% of oxygenated C₁₅-C₂₀ dimers (O:C \geq 0.4) and 70% of
90 C₁₅-C₁₉ dimer esters in SOA from α -pinene ozonolysis. However, currently the direct probing of
91 the molecular identities and chemistry of monoterpene-derived acyl RO₂ radicals is rather limited.
92 The role of acyl RO₂ in HOM formation remains to be quantified.

93 In this study, the molecular identities and formation mechanisms of acyl RO₂ radicals, as well as
94 their contributions to HOM formation in the α -pinene ozonolysis are investigated. The experiments
95 were conducted in a flow reactor with different concentrations of NO₂, which acted as an efficient
96 scavenger for the acyl RO₂. The molecular composition and abundance of the gas-phase HOMs
97 were measured by a chemical ionization-atmospheric pressure interface-time-of-flight mass
98 spectrometer (CI-APi-TOF) using nitrate as the reagent ions. In addition, kinetic modelling using
99 the Framework for 0-D Atmospheric Modeling (F0AM v4.1) employing Master Chemical
100 Mechanisms (MCM v3.3.1) updated with the latest advances of the RO₂ chemistry was performed

101 to gain insights into the reaction kinetics and mechanisms of acyl RO₂ species. We find that acyl
102 RO₂ account for a major fraction of highly oxygenated C₇ and C₈ RO₂ and play a significant role in
103 the formation of HOM monomers and dimers with small molecular size. This study will help to
104 understand the role of acyl RO₂ in the formation of low-volatility species from monoterpene
105 oxidation and reduce the uncertainties in the future atmospheric modelling of the formation and
106 impacts of aerosols.

107 **2. Method and Materials**

108 **2.1 Flow Reactor Experiments.**

109 The α -pinene ozonolysis experiments were carried out under room temperature (298 K) and dry
110 conditions (relative humidity < 5%) in a custom-built flow reactor, which has been described in detail
111 previously (Yao et al. 2019). The α -pinene vapor was generated by evaporating its pure liquid (99%,
112 Sigma-Aldrich) into a flow of zero air (10.65 L min⁻¹) added to the reactor using an automated
113 syringe pump (TYD01-01-CE, Baoding Leifu Fluid Technology Co., Ltd.). The initial
114 concentrations of α -pinene ranged from 500 ppb to 3 ppm in different experiments. Ozone was
115 generated by passing a flow of ultra-high-purity (UHP) O₂ (150 mL min⁻¹, Shanghai Maytor Special
116 Gas Co., Ltd.) through a quartz tube housing a pen-ray mercury lamp (UV-S2, UVP Inc.) and its
117 concentration (45 ppb and 180 ppb under low and high O₃ conditions, respectively) was measured
118 by an ozone analyzer (Model 49i, Thermo Fisher Scientific, USA). The NO₂, acting as an acyl RO₂
119 scavenger, was derived from its standard cylinder gas (15.6 ppm, Shanghai Weichuang Standard
120 Gas Co., Ltd.) and its initial concentration ranged from 0 to 30 ppb. To validate the formation
121 mechanisms of acyl RO₂, selected experiments with the addition of NO or cyclohexane were also
122 conducted. NO was derived by its standard cylinder gas (9.8 ppm, Shanghai Weichuang Standard
123 Gas Co., Ltd.) and its initial concentration also ranged from 0 to 30 ppb. The gas-phase cyclohexane
124 (~ 500 ppm), acting as an OH scavenger, was generated by bubbling a gentle flow of UHP N₂
125 through liquid cyclohexane (LC-MS grade, CNW). The total air flow in the flow reactor was 10.8 L
126 min⁻¹ and the residence time was 25 seconds. The relatively low O₃ concentration and short reaction
127 time in the flow reactor avoid significant production of NO₃ radicals from NO₂ and O₃ and make
128 the NO₃ oxidation contribute only 0.3%-1.2% of the total α -pinene oxidation in our experiments.
129 Therefore, the NO₃ chemistry could be neglected in this study. A summary of the experimental
130 conditions is given in Tables S1 and S2 in the Supplement.

131 The gas-phase RO₂ radicals and closed-shell products were measured by a nitrate-based CI-API-
132 TOF mass spectrometer (abbreviated as nitrate-CIMS; Aerodyne Research, Inc.), and a long time-
133 of-flight mass spectrometer with a mass resolution of ~10000 Th/Th was used here. The mass

134 calibration error is below 1.8 ppm. The sheath flow, including a 2 mL min⁻¹ UHP N₂ flow containing
 135 nitric acid (HNO₃) and 22.4 L min⁻¹ zero air was guided through a PhotoIonizer X-ray (Model L9491,
 136 Hamamatsu, Japan) to generate nitrate reagent ions. The total sample flow rate was 9 L min⁻¹ during
 137 the experiments. ~~The instrument was calibrated with a sulfuric acid (H₂SO₄) calibration factor and~~
 138 ~~a mass dependent transmission efficiency.~~ The mass spectra within the m/z range of 50 to 700 were
 139 analyzed using the tofTools package developed by Junninen et al. (2010) based on Matlab. ~~After~~
 140 ~~getting the signals of the gas phase oxygenated organic molecules (OOMs), their concentration can~~
 141 ~~be calculated as follows~~ (Jokinen et al. 2012, Bianchi et al. 2019):

$$142 \quad [OOM] = C \times \frac{I_{OOM}}{I_{NO_3^-} + I_{HNO_3NO_3^-} + I_{HNO_3HNO_3NO_3^-}} \times \frac{1}{T_i} \quad (1)$$

143 ~~C is the calibration factor of H₂SO₄, with a value of 4.06 × 10⁹ molecule cm⁻³ in this study; I_X is the~~
 144 ~~detected signal of X in the unit of counts per second (cps) and most OOMs were detected as adducts~~
 145 ~~with NO₃⁻; T_i is the mass dependent transmission efficiency of the instrument determined using the~~
 146 ~~following equation by adding propanoic acid, pentanoic acid and heptanoic acid vapors to deplete~~
 147 ~~NO₃⁻ (Figure S1):~~

$$148 \quad T_i = 0.56 + 7.2 \times 10^4 / ((m/z - 498.84)^2 + 3.46 \times 10^4) \quad (2)$$

149 To clarify whether there is SOA formation in the experiments, a scanning mobility particle sizer
 150 (SMPS, TSI), which consists of an electrostatic classifier (model 3080), a long or nano differential
 151 mobility analyzer (model 3081 and 3085 for different particle sizes), and a condensation particle
 152 counter (model 3087), was used to monitor the formation of SOA particles. Except in Exp 31 where
 153 the reacted α-pinene reached 36.8 ppb and there was low SOA formation with particle mass
 154 concentrations of 5.0×10⁻⁴-5.7×10⁻³ μg m⁻³ and number concentrations of 63-395 cm⁻³, no particle
 155 formation was observed by SMPS. Therefore, the RO₂ radicals and closed-shell products would be
 156 primarily distributed in the gas-phase, with their fates negligibly influenced by the low SOA
 157 formation under these experimental conditions.

158 2.2 Kinetic Model Simulations.

159 Model simulations of RO₂ and HOM formation in selected experiments were performed to constrain
 160 the reaction kinetics and mechanisms of acyl RO₂ using FOAM v4.1 (Wolfe et al. 2016), which
 161 employs MCM v3.3.1 (Jenkin, Young and Rickard 2015) updated with the chemistry of RO₂
 162 autoxidation and cross-reactions forming HOM monomers and dimers. Newly added species and
 163 reactions to MCM v3.3.1 followed the work by Zhao et al. (2018) and Wang et al. (2021).
 164 Considering that the default MCM v3.3.1 does not include highly oxygenated acyl RO₂, we added

165 the possible formation pathways of the potential acyl RO₂ measured in this study to the model based
166 on the mechanisms proposed by Zhao et al. (2022).

167 The formation and reaction branching ratios of the two α -pinene-derived CIs are updated in the
168 model according to the recent studies (Table S3) (Wang et al. 2021, Berndt 2022, Iyer et al. 2021,
169 Clafin et al. 2018). The formation of a ring-opened C₁₀H₁₅O₄-RO₂ species (C10H15O4RBRO2 in
170 Table S3) from α -pinene ozonolysis proposed by a recent study (Iyer et al. 2021), as well as its
171 subsequent autoxidation and bimolecular reactions, is included in the model. The autoxidation rate
172 constant of the ring-opened C₁₀H₁₅O₄-RO₂ is 1 s⁻¹, and a lower limit of its molar yield (30%) was
173 used according to the recent studies (Wang et al. 2021, Meder et al. 2023) and our results (see details
174 in Section 3.3). We also added the hydrogen abstraction channel of α -pinene oxidation by OH
175 radicals according to a recent study (Shen et al. 2022). The branching ratio of this channel was set
176 to 9%, with the rest 91% being the traditional OH addition pathways. The detailed reaction pathways
177 and rate constants of RO₂ species in this channel followed the work by Shen et al. (2022), except
178 for RO₂ cross-reactions, the rates of which were not reported in that study. As the primary RO₂
179 radicals (C₁₀H₁₅O₂-RO₂) formed via the hydrogen abstraction by OH radical are least-oxidized with
180 only 2 oxygen atoms, their cross-reaction rate could be relatively low (Atkinson et al. 2007, Orlando
181 and Tyndall 2012). In the model, this rate constant was set to 1×10^{-13} cm³ molecule⁻¹ s⁻¹. For other
182 alkyl RO₂ radicals (including HOM-RO₂), their cross-reaction rate constant is assumed to be $1 \times 10^{-}$
183 12 cm³ molecule⁻¹ s⁻¹ according to Zhao et al. (2018). The dimer formation rates for these alkyl RO₂
184 are same as their cross-reaction rates.

185 In flow reactor experiments, the equilibrium formation of ROONO₂ would lead to the consumption
186 of alkyl RO₂ radicals. To account for the influence of this process on the RO₂ budget and HOM
187 formation, we included the reaction of RO₂ + NO₂ \rightleftharpoons ROONO₂ in the model, with forward and
188 reverse reaction rate constants of 7.5×10^{-12} cm³ molecule⁻¹ s⁻¹ and 5 s⁻¹, respectively (Orlando and
189 Tyndall 2012). To simplify the parameterization, the forward and reverse reaction rate constants of
190 newly added highly oxygenated acyl RO₂ with NO₂ are the same as default values in MCM v3.3.1.
191 Besides, the cross-reaction rate constants of acyl RO₂ (including acyl RO₂ + acyl RO₂ and acyl RO₂
192 + alkyl RO₂) forming monomers or dimers were both set to 1×10^{-11} cm³ molecule⁻¹ s⁻¹ (Orlando
193 and Tyndall 2012). Considering that there are large uncertainties in the dimer formation rate of RO₂,
194 a sensitivity analysis was conducted to evaluate its influence on acyl RO₂-involved HOM formation
195 by varying the rate constant from 1×10^{-13} cm³ molecule⁻¹ s⁻¹ to 1×10^{-12} cm³ molecule⁻¹ s⁻¹ for alkyl
196 RO₂ and 1×10^{-12} cm³ molecule⁻¹ s⁻¹ to 1×10^{-11} cm³ molecule⁻¹ s⁻¹ for acyl RO₂. The results show
197 that changes in dimer formation rate constants within the above ranges have no significant influence

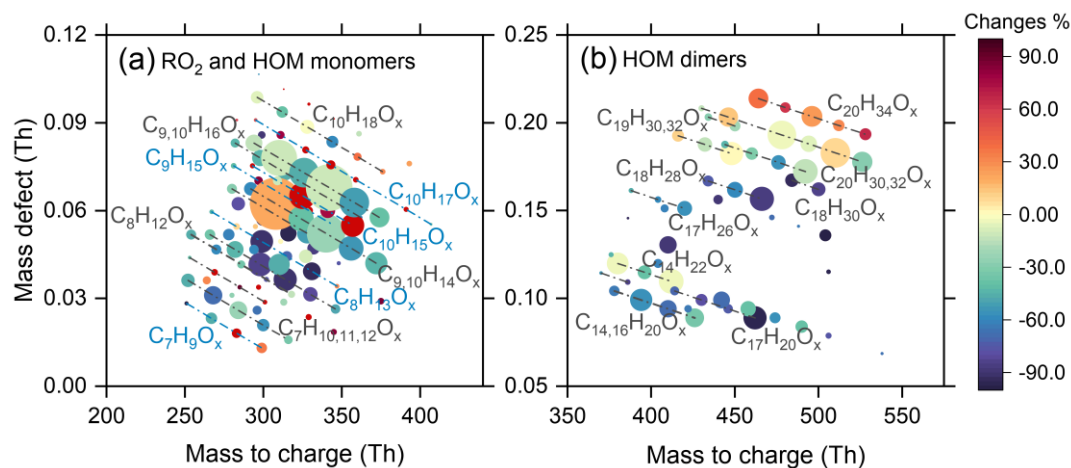
198 on the contribution of acyl RO₂ to HOM formation (Figure S2S1).

199 The wall losses of OH, HO₂, and RO₂ radicals, as well as closed-shell HOM monomers and dimers
200 in the flow reactor were considered using the KPS method proposed by Knopf et al. (2015) in the
201 model (Table S4), with an assumption of irreversible uptake of these species on the reactor wall. It
202 is found that the wall loss of OH, HO₂, and RO₂ radicals accounts for 0.08-0.14%, 4.7-9.1%, and 7.3-
203 25.5% of their total production, respectively, with lower values under higher reacted α -pinene
204 concentration conditions. Therefore, the wall loss process would not significantly influence α -
205 pinene oxidation and RO₂ chemistry. The wall losses of closed-shell HOM monomers and dimers
206 account for 18.4-34.7% and 14.2-33.1% of their total production, respectively. It should be noted
207 that the wall losses of typical RO₂ and HOMs have negligible impact on their responses to the
208 addition of NO₂ (Figure S3S2). In addition, with the consideration of the wall loss effects, the effect
209 and contribution of acyl RO₂ to the HOM formation only changed a little (0.02-0.5%). Therefore,
210 the wall losses of RO₂ and HOMs in the flow reactor would not affect the interpretation of the results
211 in this study.

212 3. Results and Discussion

213 3.1 Molecular composition of acyl RO₂ from α -pinene ozonolysis

214 The overall formation characteristics of gas-phase RO₂, closed-shell monomers, and dimers with
215 the addition of NO₂ (30 ppb) is shown in Figure 1 (Exps 8 and 14, Table S1). Since nitrate-CIMS is
216 only highly sensitive to the highly oxygenated species, we only discuss the production of HOMs
217 with oxygen atoms above 6 here. As for RO₂ and closed-shell monomers (Figure 1a), the
218 ~~concentrations-signals~~ of C₇ and C₈ species decrease by more than 50% with the addition of NO₂,
219 while for C₉ and C₁₀ species, their decreases are relatively small (within 40%). In addition, we note
220 that there is an unexpected increase in some C₉ and C₁₀ RO₂, and the possible reason will be
221 discussed in detail in Section 3.3.



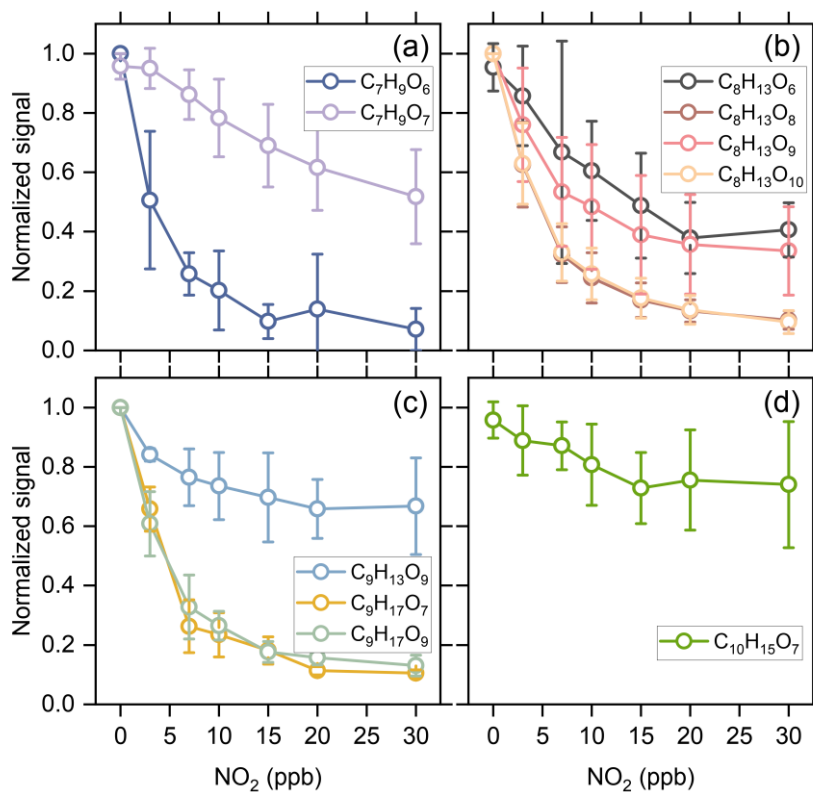
222

223 Figure 1 Mass defect plots of (a) RO₂, HOM monomers, and (b) HOM dimers formed from
 224 ozonolysis of α -pinene in the presence of NO₂ measured using nitrate-CIMS (Exps 8, 14). The
 225 circles are colored by the relative changes in concentration-signal of RO₂, monomers and dimers
 226 due to the addition of NO₂ (30 ppb). The area of circles is linearly scaled with the cube root of the
 227 concentration-signal of HOMs formed in the absence of NO₂. The blue lines represent RO₂ radicals.

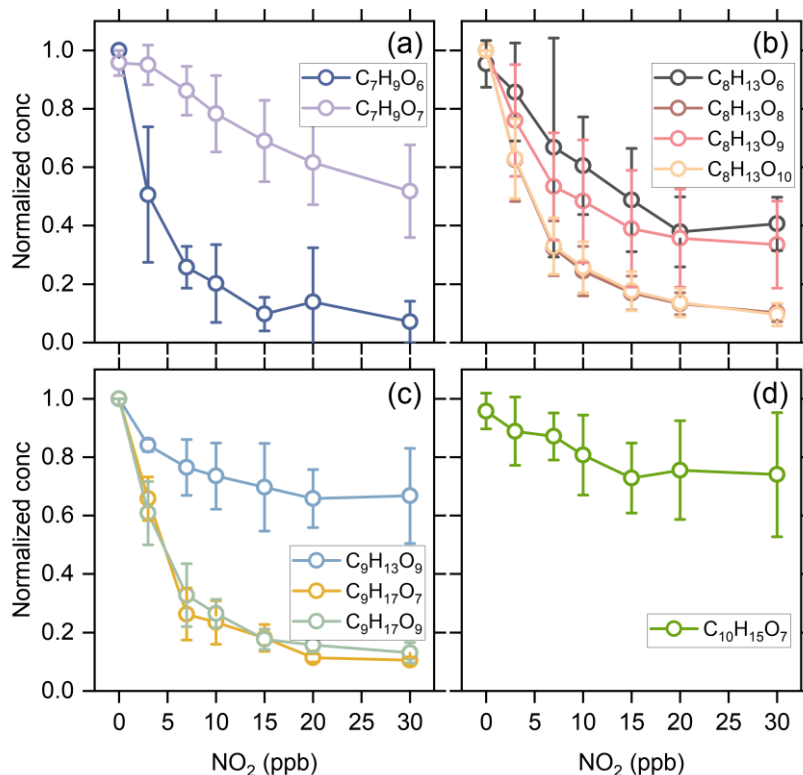
228 NO₂ could react rapidly with acyl RO₂ radicals to form RC(O)OONO₂, which has a higher thermal-
 229 stability compared to ROONO₂ and can serve as a sink for acyl RO₂ on our experimental timescales.
 230 Therefore, a significant decrease in C₇ and C₈ RO₂ and HOMs upon the addition of NO₂ indicates
 231 that a major fraction of C₇ and C₈ RO₂ are acyl RO₂. In contrast, the slight decrease in C₉ and C₁₀
 232 HOM monomers shows that the contribution of acyl RO₂ to C₉ and C₁₀ RO₂ is relatively small.
 233 However, some of the C₁₀ monomers showed a slight increase with the addition of NO₂, especially
 234 for C₁₀H₁₈O_x-HOMs. The addition of NO₂ plays a twofold role in dimer formation from α -pinene
 235 ozonolysis (Figure 1b). There is a significant inhibiting effect on C₁₄-C₁₈ dimers, which is due to
 236 the large contribution of acyl RO₂ to the total C₇ and C₈ RO₂ that generate such dimers. However,
 237 C₁₉ and C₂₀ dimers only show a slight decrease with the addition of NO₂, and some of them are even
 238 enhanced. In particular, the enhancement in C₂₀H₃₄O_x is most significant, reaching 30%.

239 Kinetic model simulations show that the concentration of alkyl RO₂ decreases by 1-20% with the
 240 addition of 30 ppb NO₂ under different reacted α -pinene conditions (Exps 1-28). Considering that
 241 the acyl RO₂ could be rapidly consumed by NO₂, if the concentration-signal reduction of a RO₂
 242 species significantly exceeds 20% with 30 ppb NO₂ addition, we presume it has significant
 243 contribution from acyl RO₂. As a result, a total of 10 acyl RO₂ were identified according to the
 244 changes of RO₂ concentration-signal as a function of initial NO₂ concentration, which include
 245 C₇H₉O₆, C₇H₉O₇, C₈H₁₃O₆, C₈H₁₃O₈, C₈H₁₃O₉, C₈H₁₃O₁₀, C₉H₁₃O₉, C₉H₁₇O₇, C₉H₁₇O₉, and
 246 C₁₀H₁₅O₇. Figure 2 shows the averaged normalized acyl RO₂ concentrations-signals measured as a

247 function of the added NO_2 concentration under different experimental conditions (Exps 1-28).
 248 Similarly, since nitrate-CIMS is only highly sensitive to products with high oxygen content, we only
 249 observed acyl RO_2 with oxygen atoms above 6. Consistent with the significant decrease in C_7 and
 250 C_8 species with the addition of NO_2 in Figure 1a, C_7 and C_8 acyl RO_2 decrease by more than 50%
 251 with the increase of NO_2 concentration (Figures 2a, b). For C_9 acyl RO_2 , the $\text{C}_9\text{H}_{17}\text{O}_7\text{-RO}_2$ and
 252 $\text{C}_9\text{H}_{17}\text{O}_9\text{-RO}_2$ also decrease dramatically with increasing NO_2 , and the decrease in $\text{C}_9\text{H}_{13}\text{O}_9\text{-RO}_2$ is
 253 relatively smaller (Figure 2c). In addition, $\text{C}_{10}\text{H}_{15}\text{O}_7\text{-RO}_2$ also shows a small decrease (Figure 2d),
 254 with a reduction of only 30% at 30 ppb NO_2 . The relatively small reduction in the abundance
 255 of some of these RO_2 radicals indicates the presence of alkyl RO_2 radicals with the same chemical
 256 formulas. Along with the marked reduction in acyl RO_2 signals, the production of highly oxygenated
 257 RC(O)OONO_2 species such as $\text{C}_9\text{H}_{13}\text{O}_9\text{NO}_2$, $\text{C}_9\text{H}_{17}\text{O}_7\text{NO}_2$, and $\text{C}_{10}\text{H}_{15}\text{O}_7\text{NO}_2$ with the addition of
 258 NO_2 were observed (see the spectra in Figure S3). However, we note that although some
 259 RC(O)OONO_2 such as $\text{C}_8\text{H}_{13}\text{O}_6\text{NO}_2$ and $\text{C}_8\text{H}_{13}\text{O}_8\text{NO}_2$ are expected to be formed with NO_2 addition,
 260 they could not be unambiguously detected by nitrate-CIMS due to the overlapping of their peaks
 261 with strong alkyl RO_2 peaks ($\text{C}_9\text{H}_{15}\text{O}_8\text{-RO}_2$ and $\text{C}_9\text{H}_{15}\text{O}_{10}\text{-RO}_2$) in this study.



264



265

266 Figure 2 Averaged normalized concentration-signal of the measured acyl RO₂ as a function of the
 267 added NO₂ concentration under different experimental conditions (Exps 1-28).

268 Figure 3 shows the contribution of acyl and alkyl RO₂ to the highly oxidized C₇-C₁₀ RO₂. Acyl RO₂
 269 contribute 67.266.9%, 94.3% and 31.931.7% to the total C₇, C₈, and C₉ RO₂ concentrationssignals,
 270 respectively. By contrast, the only C₁₀ acyl RO₂ measured in this study is C₁₀H₁₅O₇, which
 271 contributes to only 0.50.4% of the total C₁₀ RO₂. It should be note that there might be other C₁₀ acyl
 272 RO₂ that were not observed due to the interferences from the alkyl RO₂ with the same chemical
 273 formulas, which respond differently to the addition of NO₂ than acyl RO₂ do (see details in the
 274 following discussion). Considering that some RO₂ formulas such as C₁₀H₁₅O₇ may have
 275 contributions from both acyl RO₂ and alkyl RO₂, we assumed the decrease of RO₂ concentration
 276 signal with the addition of NO₂ as the concentration-signal of acyl RO₂. Besides, it is obvious that
 277 the normalized concentration-signal basically decreases to the lowest value when the initial NO₂
 278 concentration reaches 10 ppb (Figure 2), indicating that most of the acyl RO₂ are depleted at this
 279 NO₂ concentration. In addition, the decreasing extents of some acyl RO₂ are different for different
 280 reacted α -pinene concentrations, with lower decreasing extent for higher reacted α -pinene
 281 concentrations (Figure S4S54). This difference might be due to the promoted cross-reactions of acyl
 282 RO₂ as well as their precursor RO₂ at higher α -pinene concentrations, which are competitive with
 283 the reactions leading to acyl RO₂ formation as well as the acyl RO₂ + NO₂ reactions.

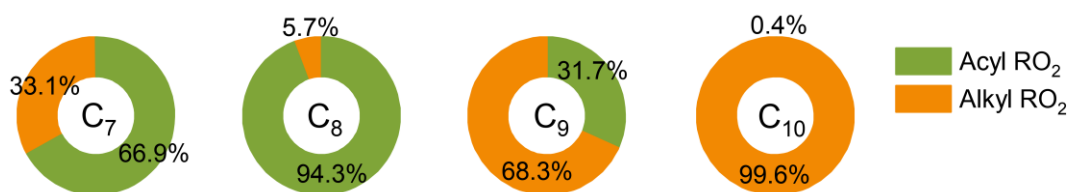


Figure 3 Contributions of acyl and alkyl RO₂ to the highly oxygenated C₇-C₁₀ RO₂ measured by nitrate-CIMS.

In addition to the changes of acyl RO₂ [concentration-signal](#), we also show the changes of normalized alkyl RO₂ [concentration-signal](#) with the increasing initial NO₂ concentration in Figure [S5S65](#). Although ROONO₂ formed by the reaction of alkyl RO₂ with NO₂ is thermally unstable and would decompose quickly to release RO₂, it would still reach a formation/decomposition equilibrium in the system, thus consuming a small amount of alkyl RO₂. However, it can be seen from Figure [S5S65](#) that during 25 s of reaction in the flow reactor, a large part of alkyl RO₂ has an increasing trend with the increase of NO₂ concentration. We speculate that a portion of ROONO₂ could decompose back to RO₂ and NO₂ in the nitrate-CI inlet where the sample gases were diluted instantly and the equilibrium of ROONO₂ was disturbed, resulting in the release of a large amount of RO₂.

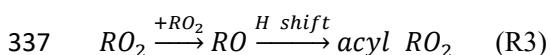
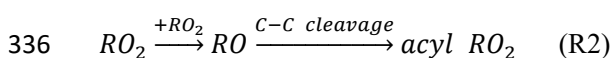
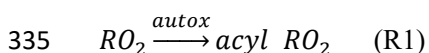
To verify our speculation, the decomposition of ROONO₂ in the CI inlet was simulated based on the dilution ratio (1:3.5) and residence time (200 ms) in the inlet. As shown in Figure [S6S76](#), more than 40% of ROONO₂ decompose back to RO₂ and NO₂ in the CI inlet, which would inevitably lead to an increase in RO₂ concentration. As the C₁₀H₁₅O₈NO₂ has a significant contribution from the relative stable RC(O)OONO₂ arising from the ring-opened acyl C₁₀H₁₅O₈-RO₂ reported by Iyer et al. (2021), its decomposition is relatively small (~21%). It should be noted that the RO₂ measured here is only a part of total RO₂ and that a large amount of RO₂ has already reacted to form closed-shell products as well as ROONO₂ in the flow reactor. Taking Exp 14 as an example (30 ppb NO₂), the simulated concentrations of RO₂ and ROONO₂ are 1.3 ppb and 1.9 ppb, which approximately accounts for 27.1% and 39.6% of the total production of RO₂, respectively. Therefore, the decomposition of ROONO₂ could indeed result in an increase in the RO₂ [concentration-signal](#). It should also be pointed out that because of the very short residence time in the CI inlet, such an increase in the RO₂ concentration would not significantly impact HOM formation.

To confirm the reliability of our results, we examined the changes in the [concentration-signals](#) of RO₂ and closed-shell products as a function of reacted α -pinene in the absence of NO₂ (Section S1 and Figure [S7S78](#)), and the results are consistent with previous studies (Zhao et al. 2018). In addition, we repeated Exps 15-21 on another nitrate-CIMS and a similar increase in alkyl RO₂ signals with the addition of NO₂ was observed on that instrument (Figure [S8S989](#)).

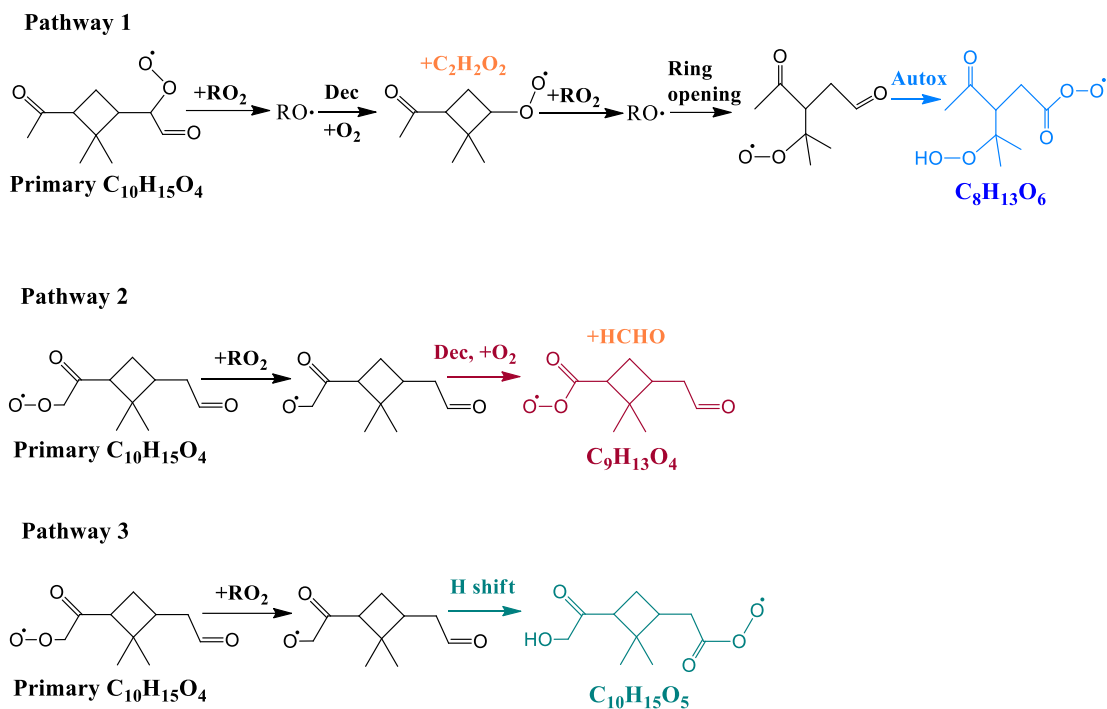
315 3.2 Formation mechanisms of acyl RO₂ during α -pinene ozonolysis

316 It has been recently suggested that there are three main pathways that directly lead to the formation
317 of monoterpene-derived acyl RO₂ (Zhao et al. 2022) (Shen et al. 2022): (i) the autoxidation of RO₂
318 containing aldehyde groups (Reaction R1), (ii) the cleavage of C-C bond of RO containing an α -
319 ketone group (Reaction R2), and (iii) the intramolecular H-shift of RO containing an aldehyde group
320 (Reaction R3). In addition, the secondary OH oxidation of aldehyde products can also produce acyl
321 RO₂ radicals. However, in the present study, the secondary OH oxidation is expected to be
322 insignificant due to an excess of α -pinene compared to O₃. Indeed, kinetic model simulations
323 incorporating the secondary OH chemistry show that the contribution of secondary OH oxidation to
324 acyl RO₂ formation is negligible even under high O₃ conditions (see details in Section S2 and Figure
325 S910).

326 Here, we further investigated the formation mechanisms of acyl RO₂. Figure 4 shows the reaction
327 schemes leading to the formation of example acyl RO₂ radicals. The detailed formation mechanisms
328 of acyl RO₂ measured in this study are shown in Figure S9S101. The formation of acyl RO₂,
329 especially those having the small molecular size (C₇-C₉), requires the production and subsequent
330 decomposition (or ring-opening process) of RO radicals. Take C₈H₁₃O₆-RO₂ as an example (Figure
331 4), two steps of RO formation and decomposition following the primary C₁₀H₁₅O₄-RO₂ lead to the
332 ring-opened C₈H₁₃O₄-RO₂ that can undergo rapid aldehydic H-shift to form the acyl RO₂. While for
333 C₈H₁₃O₉-RO₂, it directly comes from the aldehydic H-shift of C₈H₁₃O₇-RO followed by the O₂
334 addition (Figure S9S101).

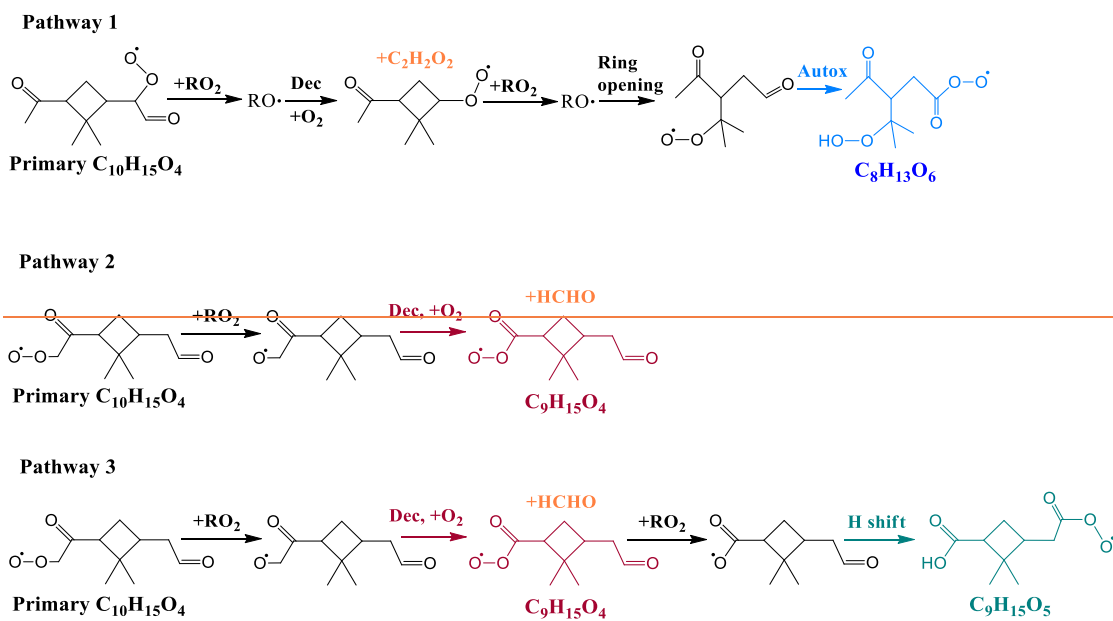


338



339

340 Figure 4 Three different formation pathways of acyl RO_2 during ozonolysis of α -pinene. The acyl
 341 RO_2 , $C_9H_{15}O_4$, $C_9H_{13}O_4$ and $C_9H_{15}O_5$, $C_{10}H_{15}O_5$, formed via pathways 2 and 3, respectively, were not
 342 detected by nitrate-CIMS in this study due to their relatively low oxygenation level.

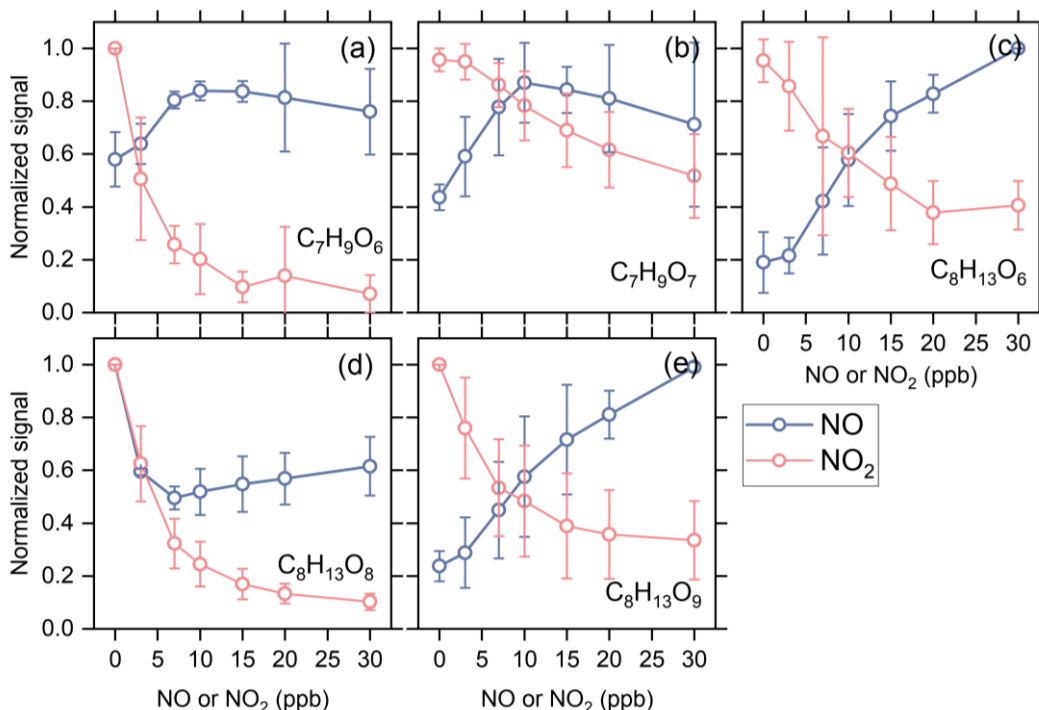


343

344 ~~Figure 4 Three different formation pathways of acyl RO_2 during ozonolysis of α -pinene. The acyl~~
 345 ~~RO_2 , $C_9H_{15}O_4$, $C_9H_{13}O_4$ and $C_9H_{15}O_5$, $C_{10}H_{15}O_5$, formed via pathways 2 and 3, respectively, were not~~
 346 ~~detected by nitrate-CIMS in this study due to their relatively low oxygenation level.~~

347 To verify the formation mechanisms of acyl RO_2 , we added NO in some experiments (Exps 33-56)

348 to see how acyl RO₂ respond to the increasing NO concentration. As shown in Figure 5, the changes
 349 of C₇ and C₈ acyl RO₂ show opposite trend with the increasing NO and NO₂ concentration, except
 350 for C₈H₁₃O₈-RO₂. NO can react with RO₂ to form RO radicals and promote the formation of RO₂
 351 that requires the involvement of RO radicals in their formation. In addition to C₈H₁₃O₆-RO₂
 352 discussed above, the formation of C₇H₉O₇-RO₂ and C₈H₁₃O₉-RO₂ needs 2 and 4 steps of the RO
 353 formation following C₁₀H₁₅O₄-RO₂ (Figure S9S1+04), respectively. Therefore, the increase of RO
 354 concentration due to the addition of NO would promote the production of these acyl RO₂. These
 355 results prove that the RO radicals indeed play an important role in the acyl RO₂ formation. While
 356 for C₈H₁₃O₈-RO₂, its concentration-signal decreases substantially with the addition of NO up to 3
 357 ppb, similar to the trend observed with the addition of NO₂. After reaching the minimum at 7 ppb
 358 NO, the concentration-signal of C₈H₁₃O₈-RO₂ tends to increase with the further increase of NO
 359 concentration. Given that C₈H₁₃O₈-RO₂ is likely to directly come from the autoxidation of C₈H₁₃O₆
 360 acyl RO₂ (see Figure S9S1+04), the rapid consumption of C₈H₁₃O₆-RO₂ by NO and NO₂ (formed
 361 by O₃ oxidation of NO) may outcompete its autoxidation process, thus leading to a decrease in
 362 C₈H₁₃O₈-RO₂ concentrationsignal. Besides, it can be seen that the increasing extent in C₈H₁₃O₆-
 363 RO₂ is also relatively small before the NO concentration reaches 3 ppb (Figure 5c), indicating that
 364 the promotion effect of NO on C₈H₁₃O₆-RO₂ formation is not that strong at this concentration.

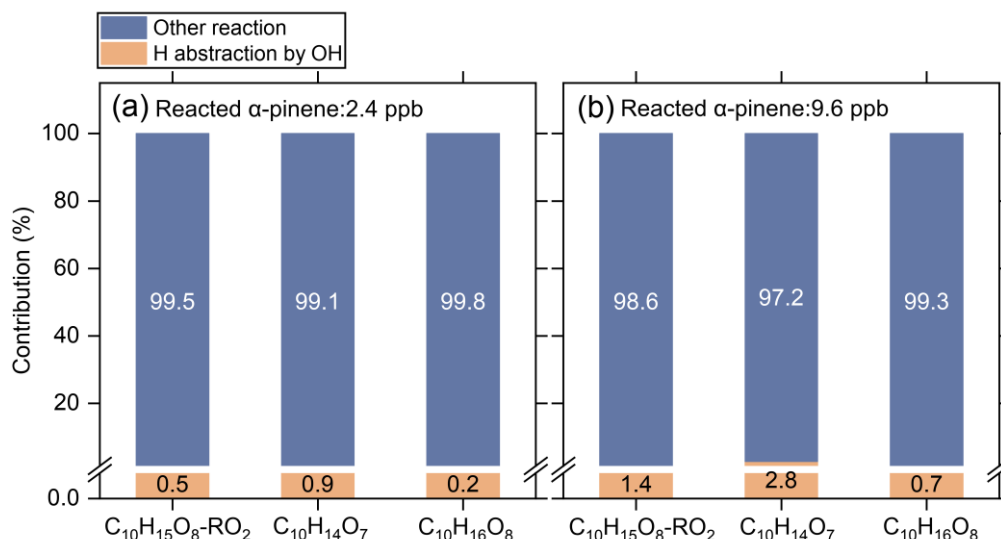


365
 366 Figure 5 Averaged normalized concentration-signal of typical acyl RO₂ as a function of initial NO
 367 or NO₂ addition (Exps 1-28 and 33-56).

368 It is interesting to note that most of the measured highly oxygenated acyl RO₂ are formed by the

369 autoxidation of aldehydic RO₂, and only the C₈H₁₃O₉-RO₂ is formed by the H-shift of the RO radical
370 (Figure S9S1104). The ~~measured concentration signal~~ of acyl RO₂ from the autoxidation pathway
371 accounts for 96% of all highly oxygenated acyl RO₂ ~~concentrations signals~~. Considering that the
372 acyl RO₂ with small molecular size are generally the ring-opened RO₂, the autoxidation rate constant
373 of their precursor RO₂ is expected to be relatively high (e.g., 1 s⁻¹) (Iyer et al. 2021). Taking a RO₂
374 cross-reaction rate constant of 1 × 10⁻¹² cm³ molecule⁻¹ s⁻¹ (Zhao et al. 2018) and a model-predicted
375 total RO₂ concentration of 1.7 ppb (Exp 8), ~~the simulated contributions of~~ autoxidation and cross-
376 reactions ~~contribute to 96.0% and 4.0% of~~ the total RO₂ reaction ~~are 96.0% and 4.0%~~, respectively.
377 Considering a 10 times larger RO₂ cross-reaction rate constant (i.e., 1 × 10⁻¹¹ cm³ molecule⁻¹ s⁻¹),
378 the ~~simulated~~ contributions of RO₂ autoxidation and cross-reactions would be 70.4% and 29.6%,
379 respectively. These ~~calculations simulations~~ suggest that the autoxidation of aldehydic RO₂ plays a
380 dominant role in the formation of the highly oxygenated acyl RO₂. Although the acyl RO₂ with low
381 oxygen content were not measured in this study, all acyl RO₂ containing oxygen atoms less than 6
382 seem to be derived from the cleavage of C-C bond or H-shift of RO containing an α-ketone or
383 aldehyde in the currently known reaction mechanisms (Figures 4 and S10S1212).

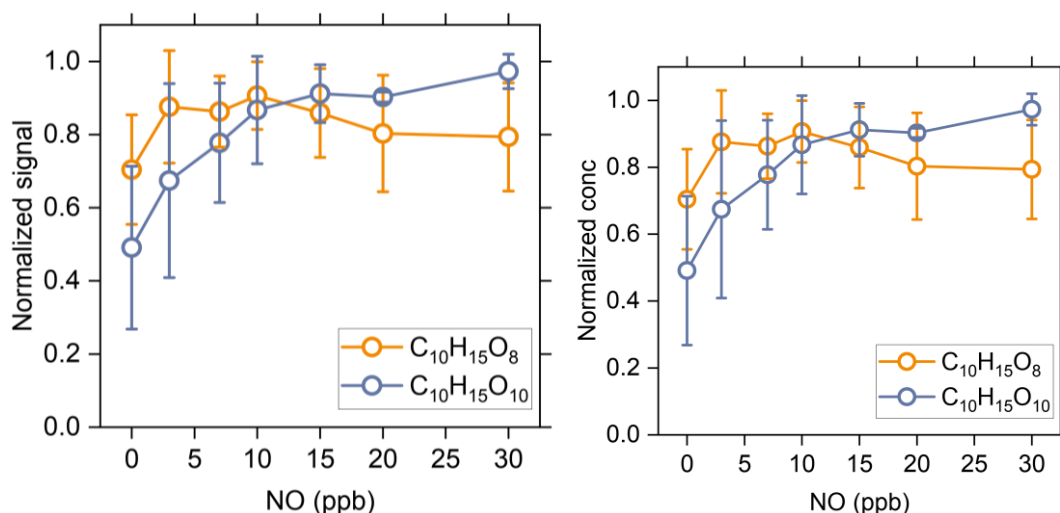
384 Recently, Shen et al. (2022) found that the hydrogen abstraction by OH radicals during α-pinene
385 oxidation plays an important role in HOM formation. In such mechanisms, the primary RO₂ reacts
386 with NO and forms RO radicals, which could undergo rapid ring-breaking reactions to form a series
387 of ring-opened C₁₀H₁₅O_x-RO₂, which contains aldehyde functionality and can easily autoxidize to
388 C₁₀ acyl RO₂. In the absence of NO, the cross-reactions of RO₂ can also produce RO radicals.
389 However, only a few C₁₀ acyl RO₂ were detected in this study and they contribute less than 1% of
390 the total C₁₀ RO₂ concentration. This phenomenon could be due to the fact that the primary RO₂
391 (C₁₀H₁₅O₂) formed by the hydrogen abstraction by OH radical are least-oxidized with only 2 oxygen
392 atoms, which are expected to have a relatively low cross-reaction rate constant (Berndt et al. 2018,
393 Orlando and Tyndall 2012). As a result, the formation of ring-opened C₁₀H₁₅O_x-RO₂ via cross-
394 reactions of the primary C₁₀H₁₅O₂-RO₂ may not be important. As shown in Figure 6, when the cross-
395 reaction rate constants of C₁₀H₁₅O₂-RO₂ is considered to be 1 × 10⁻¹³ cm³ molecule⁻¹ s⁻¹, the
396 simulated contribution of the H-abstraction pathway to the HOM formation is less than 3% under
397 both low (2.4 ppb) and high (9.6 ppb) reacted α-pinene conditions. It should be note that the cross-
398 reaction rate constants of the less-oxygenated RO₂ could be even lower (Orlando and Tyndall 2012),
399 therefore the contribution of this pathway to HOM formation could be ignored when NO is absent.



400

401 Figure 6 Contributions of the H-abstraction pathways by OH radicals (yellow) and OH addition and
 402 ozonolysis pathways (blue) to the formation of typical HOMs under low (a) and high (b) reacted α -
 403 pinene conditions simulated by the kinetic model. The cross-reaction rate constant was set to $1 \times$
 404 $10^{-13} \text{ cm}^3 \text{ molecule}^{-1} \text{ s}^{-1}$ for the primary $C_{10}H_{15}O_2-RO_2$ and $1 \times 10^{-12} \text{ cm}^3 \text{ molecule}^{-1} \text{ s}^{-1}$ for the more
 405 oxygenated RO_2 .

406 In the presence of cyclohexane as an OH scavenger (Figure S11S1323, Exp 32), the measured
 407 concentrations-signals of $C_{10}H_{17}O_x-RO_2$ formed via OH addition channel and the corresponding
 408 $C_{10}H_{18}O_x$ -HOMs decrease by more than 70%, while the $C_{10}H_{15}O_x-RO_2$ and its related closed-shell
 409 products decrease by less than 15%, in good agreement with the measurements in previous studies
 410 (Zhao et al. 2018). As the $C_{10}H_{16}O_8$ -HOM could come from both $C_{10}H_{15}O_x-RO_2$ and $C_{10}H_{17}O_x-RO_2$,
 411 its reduction is at a medium level. The significantly smaller decrease in the concentrations-signals
 412 of $C_{10}H_{15}O_x-RO_2$ and its corresponding closed-shell products as compared to those of $C_{10}H_{17}O_x$ -
 413 RO_2 and the related closed-shell products further illustrates that the H-abstraction by OH has a minor
 414 contribution to HOM formation in the absence of NO.



415

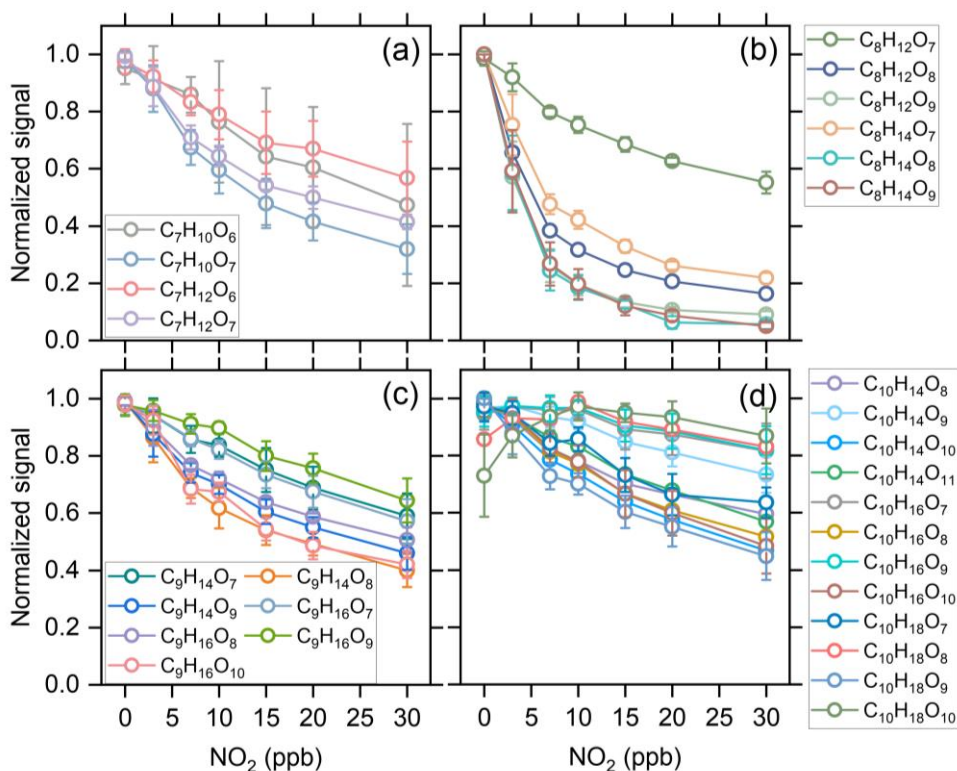
416 Figure 7 Averaged normalized concentration-signal of the measured C₁₀H₁₅O₈- and C₁₀H₁₅O₁₀-
 417 RO₂ as a function of the added NO concentration (Exps 33-56).

418 Figure 7 shows the changes in measured concentration-signal of C₁₀H₁₅O₈-RO₂ and C₁₀H₁₅O₁₀-RO₂
 419 as a function of initial NO concentration (Exps 33-56). It should be noted that due to the existence
 420 of O₃ in our experiments, these two RO₂ could come from both O₃ and OH reactions with α-pinene
 421 and NO could be rapidly oxidized to NO₂ by O₃. The normalized concentrations-signals of
 422 C₁₀H₁₅O₈-RO₂ and C₁₀H₁₅O₁₀-RO₂ increase firstly under low NO conditions, which is similar to the
 423 change of acyl RO₂ as shown in Figure 5. This increase could be due to two reasons: (1) the
 424 promoted formation of C₁₀H₁₅O₈ and C₁₀H₁₅O₁₀ acyl RO₂ from the H-abstraction channel by NO
 425 addition and (2) the equilibrium decomposition of ROONO₂ formed by the two alkyl RO₂ from
 426 ozonolysis of α-pinene in the CI inlet (see Section 3.1). As mentioned above, the ring-opened
 427 C₁₀H₁₅O_x-RO₂ formed from the H-abstraction channel contain aldehyde functionality and can
 428 autoxidize rapidly. The F0AM model simulations show that the C₁₀H₁₅O₈ and C₁₀H₁₅O₁₀ acyl RO₂
 429 formed from the H-abstraction channel contribute to 68% and 56% of the total C₁₀H₁₅O₈-RO₂ and
 430 C₁₀H₁₅O₁₀-RO₂ with the addition of 10 ppb NO, respectively. Therefore, the initial increases of these
 431 two RO₂ with increasing NO concentration are likely mainly due to the enhanced formation of
 432 C₁₀H₁₅O₈ and C₁₀H₁₅O₁₀ acyl RO₂. When the NO concentration increases to a high level, there are
 433 more NO and NO₂ in the system, which promotes the consumption of acyl RO₂. As a result,
 434 C₁₀H₁₅O₈-RO₂ exhibits a decreasing trend and the increasing extend of C₁₀H₁₅O₁₀-RO₂ becomes
 435 much smaller.

436 3.3 Contributions of acyl RO₂ to the formation of gas-phase HOMs

437 With the addition of NO₂, the distribution of gas-phase products in the α-pinene ozonolysis changes
 438 significantly (see Figure 1), and the consumption of acyl RO₂ by NO₂ plays an important role. NO₂

439 influences the formation of HOM monomers mainly in three ways. Firstly, NO_2 could react rapidly
 440 with acyl RO_2 and form RC(O)OONO_2 , thus inhibiting the formation of HOMs with the
 441 involvement of acyl RO_2 . Secondly, as mentioned above, although ROONO_2 is thermally unstable,
 442 their formation/decomposition equilibrium still consumes a small amount of alkyl RO_2 , resulting in
 443 a decrease in HOM formation. Thirdly, NO_2 can consume a part of HO_2 radicals (Figure S12S1434,
 444 thus inhibiting the $\text{RO}_2 + \text{HO}_2$ reaction pathway.



445
 446 Figure 8 Averaged normalized concentration-signal of the measured C_7 - C_{10} HOMs as a function of
 447 the added NO_2 concentration (Exps 1-28).

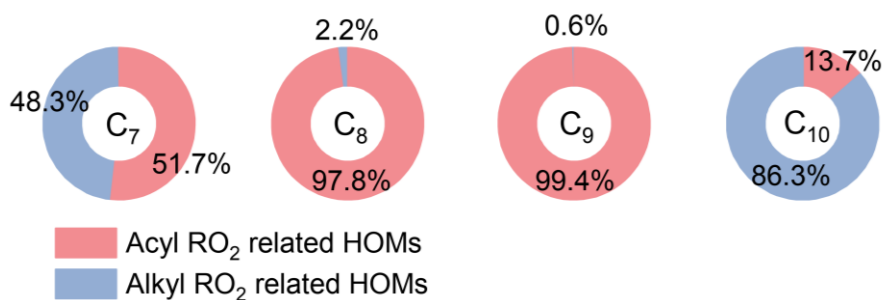
448 Figure 8 shows the normalized concentration-signal of C_7 - C_{10} HOM monomers as a function of
 449 initial NO_2 concentration. The C_7 , C_8 , and some of C_9 HOMs decrease significantly with increasing
 450 NO_2 concentration due to the relatively large contribution of acyl RO_2 to the total C_7 - C_9 RO_2 . The
 451 C_7 HOMs decrease by more than 50% when the NO_2 concentration reaches 30 ppb, while C_8 HOMs
 452 decrease by more than 70% and some of them even decrease by 90%. The C_9 HOMs decrease by
 453 30%-60% and the species with relatively large decrease are mostly acyl RO_2 -related HOMs. For
 454 C_{10} HOMs, although there is also an obvious decrease in their formation with the addition of NO_2 ,
 455 most of them have a smaller decreasing extent compared to the C_7 - C_9 HOMs due to the low
 456 contribution of acyl RO_2 to the C_{10} RO_2 . It is worth noting that a few C_{10} HOMs increase initially
 457 with the addition of NO_2 up to 10 ppb, suggesting that there might be some processes that promote
 458 the formation of their precursor RO_2 radicals and thus offset the inhibiting effect of NO_2 .

459 As mentioned above, the addition of NO₂ has the most significant influence on the formation of
460 small HOM monomers. Combined with the large contribution (67-94%) of acyl RO₂ to the total C₇
461 and C₈ RO₂ (Figure 3), it can be considered that the reduction in the formation of C₇ and C₈ HOM
462 monomers with NO₂ addition is overwhelmingly due to the consumption of acyl RO₂ by NO₂. As a
463 result, acyl RO₂ was found to have a contribution of 50-90% to C₇ and C₈ HOM monomer formation
464 during α -pinene ozonolysis. Since acyl RO₂ also have a considerable contribution (32%) to the total
465 C₉ RO₂, an upper limit (30%-60%) of its contribution to C₉ HOMs could be derived with the
466 assumption that the decrease of C₉ HOMs with the addition of NO₂ is also mainly due to the
467 consumption of C₉-acyl RO₂ by NO₂. By contrast, acyl RO₂ account for a very small fraction (0.54%)
468 of the total C₁₀ RO₂, and their contribution to C₁₀ HOMs cannot be quantified based solely on the
469 experimental measurements given that the equilibrium reaction between alkyl RO₂ and NO₂ can
470 also affect the formation of HOMs. Therefore, we used the FOAM model to simulate the contribution
471 of acyl RO₂ to C₁₀ HOM formation according to the acyl RO₂ measured in this study and displayed
472 the results in Figure 9. It should be noted that the HOMs from the acyl RO₂ and its subsequent RO₂
473 (formed from acyl RO₂ reactions) are all considered as acyl RO₂-related HOMs in the model.

474 As mentioned above, the formation of ring-opened C₁₀H₁₅O₄-RO₂ reported by Iyer et al. (2021) is
475 included in the model, and its autoxidation produces a ring-opened acyl C₁₀H₁₅O₈-RO₂. When we
476 considered the upper limit of the yield of ring-opened C₁₀H₁₅O₄-RO₂ (89%) in the model and
477 assumes that the other primary RO₂ with the cyclobutyl ring autoxidize at a very slow rate (0.01 s⁻¹),
478 the simulated acyl C₁₀H₁₅O₈-RO₂ would contribute to ~80% of the total C₁₀ RO₂. However, we
479 could not see a large decrease in the measured ~~concentration-signal~~ of C₁₀H₁₅O₈-RO₂ and its related
480 HOM monomers with the addition of NO₂. Similarly, a recent study by Zhao et al. (2022) found
481 that the C₁₀H₁₅O₈-related monomers and dimers in α -pinene SOA ~~also~~ did not ~~show~~ significantly
482 decreases with NO₂ addition. There might be ~~two~~-~~three~~ reasons for the discrepancy between the
483 simulations and measurements. Firstly, the yield of the ring-opened C₁₀H₁₅O₄-RO₂ might be
484 significantly smaller than 89% (Wang et al. 2021, Meder et al. 2023). Secondly, the autoxidation
485 rate of other primary C₁₀H₁₅O₄-RO₂ with the cyclobutyl ring could be significantly larger than 0.01
486 s⁻¹. Thirdly, the ring-opened C₁₀H₁₅O₈-RO₂, a highly functionalized acyl RO₂ radical with an -OOH
487 group, may be able to undergo very fast intramolecular H-scrambling reactions to form a peroxy
488 acid as suggested by Knap and Jørgensen (2017), which would compete with the NO₂ reaction and
489 result in a lower reduction in its signal upon NO₂ addition (see details in Section S3).

490 To examine the contributions of acyl RO₂ to C₁₀ HOM production, ~~We~~ updated the branching
491 ratios and autoxidation rates of the primary RO₂ during ~~the~~ α -pinene ozonolysis in the model

492 according to the recent studies (Wang et al. 2021, Kurten et al. 2015, Claffin et al. 2018, Berndt
 493 2022) (Table S3), and used a lower limit (30%) of the ring-opened $C_{10}H_{15}O_4-RO_2$ yield reported by
 494 Iyer et al. (2021) ~~was used here~~. The simulated acyl RO_2 -related HOMs contribute to 14% of the
 495 total C_{10} HOMs, which is slightly smaller than the measured decrease in C_{10} HOMs with the addition
 496 of NO_2 . This discrepancy could be due to two reasons. Firstly, the decrease in HOMs can partly
 497 result from the consumption of alkyl RO_2 and HO_2 radicals by the addition of NO_2 . Secondly, as
 498 mentioned above, there might be other C_{10} acyl RO_2 that were not observed in this study due to the
 499 decomposition of the $ROONO_2$ from the alkyl RO_2 with the same formulas. The contributions of
 500 acyl RO_2 to the formation of C_7 - C_9 HOMs were also simulated (Figure 9). For C_7 and C_8 HOMs,
 501 the model predicts a contribution of 52%-98% from acyl RO_2 , which is consistent with the
 502 measurements (50%-90%). However, the simulated contribution of acyl RO_2 to C_9 HOMs is over
 503 99%, which is not consistent with the measurements (Figure 8c). Recent studies indicated that the
 504 CI radicals from α -pinene ozonolysis could not form the alkyl $C_9H_{15}O_3-RO_2$ (C_9O_2 in default
 505 MCM v3.3.1) (Berndt 2022, Wang et al. 2021, Kurten et al. 2015). As a result, this primary C_9 alkyl
 506 RO_2 was not considered in the model, and most of C_9 RO_2 considered are acyl RO_2 or from acyl
 507 RO_2 reactions. In view of the significantly lower measured (less than 30-60%) than simulated (over
 508 99%) contribution of acyl RO_2 to C_9 HOMs, we speculate that a small part of CI radicals might be
 509 able to form the $C_9H_{15}O_3-RO_2$, which could further react to form highly oxygenated alkyl C_9 RO_2 .



510

511 Figure 9 Simulated average contribution of acyl and alkyl RO_2 to C_7 - C_{10} HOM formation from
 512 ozonolysis of α -pinene under typical experimental conditions (Exps 1, 8, 15, and 22).

513

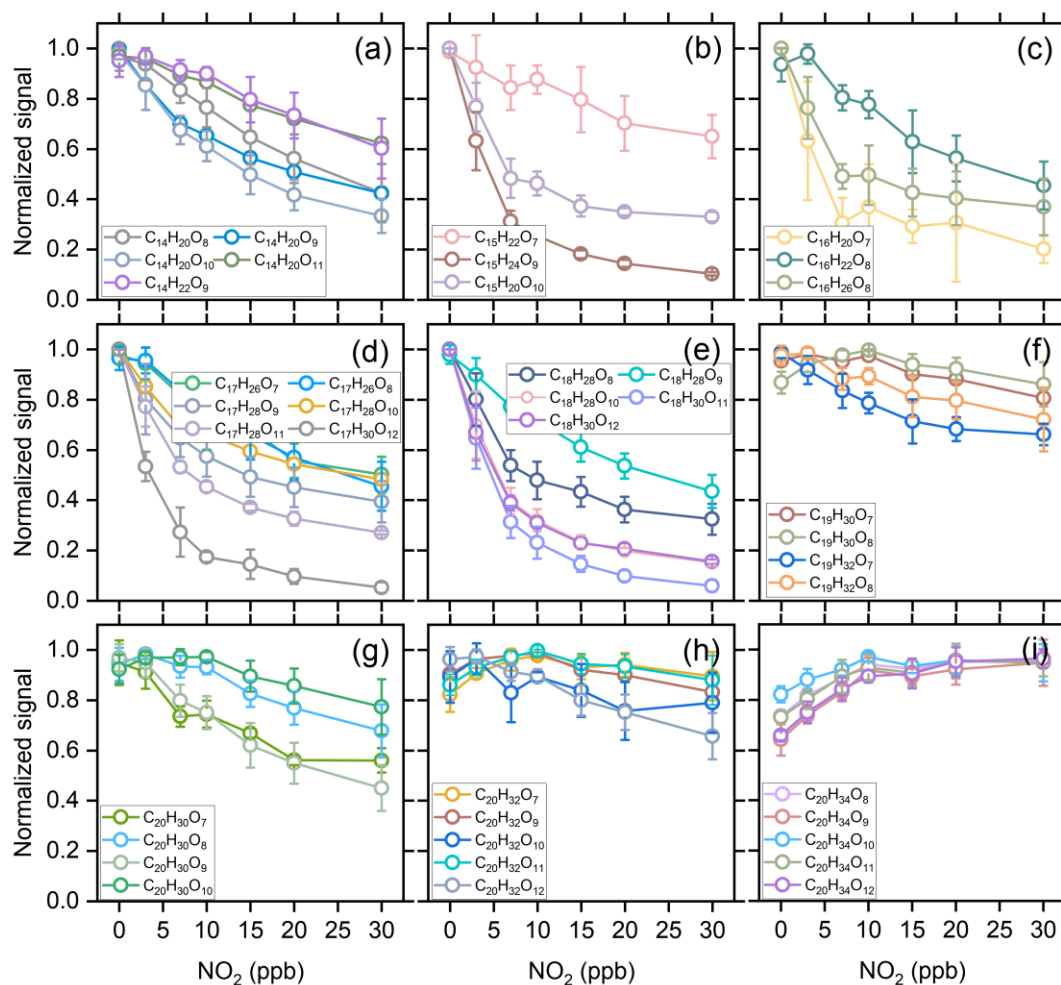
514 A sensitive-sensitivity analysis of the alkyl $C_9H_{15}O_3-RO_2$ yield was conducted to see its influence
 515 on the contribution of acyl RO_2 to the total C_9 HOMs. The model simulations show that when the
 516 yield of this C_9 RO_2 from one of the CIs ranges between 0.5% to 2%, the contribution of acyl RO_2
 517 to the total C_9 HOMs ranges from 27.5% to 59.8% (Figure ~~S13~~S155), which is almost consistent
 518 with the measurements. This result indicates that a small part of CIs could generate the C_9 alkyl
 519 RO_2 . We note that Wethe small production of $C_9H_{15}O_3-RO_2$ from CIs has no significant influence

520 on the yield of C₁₀H₁₅O₄-RO₂ and the subsequent acyl RO₂. As shown in Figure S16, as the C₉H₁₅O₃-
521 RO₂ yield increases from 0% to 3%, the simulated concentrations of C₁₀H₁₅O₄-RO₂ exhibit
522 negligible to small (5%) changes. As the C₉H₁₅O₃-RO₂ is considered to only produce highly
523 oxygenated alkyl RO₂ in the model, it results in a decrease in the contribution of acyl RO₂ to the
524 total C₉ HOMs. However, the contributions of acyl RO₂ to total C₇, C₈, and C₁₀ HOMs are almost
525 unchanged.

526 The cross-reaction rate constant of acyl RO₂ is generally larger than that of alkyl RO₂ (Orlando and
527 Tyndall 2012, Atkinson et al. 2007), and the fast cross-reaction may lead to an important
528 contribution to the HOM dimer production. The responses of dimer formation to increasing
529 concentration of initial NO₂ during α-pinene ozonolysis are given in Figure 10. The C₁₄-C₁₈ dimers
530 decrease by up to 50%-95% with the increase of NO₂ concentration up to 30 ppb (Figures 10a-e).
531 The rapid cross-reaction rate of acyl RO₂, as well as their dominant contribution to the small RO₂
532 species makes acyl RO₂ an important contributor to the formation of these dimers. The consumption
533 of acyl RO₂ by NO₂ greatly inhibits the bimolecular reactions involving acyl RO₂, resulting in a
534 rapid decrease in the ~~concentration-signal~~ of the corresponding dimers. Considering the
535 predominance of acyl RO₂ in small RO₂ and their high reaction rate with NO₂ compared to the alkyl
536 RO₂, it can be concluded that the cross-reactions involving acyl RO₂ contribute to roughly 50%-95%
537 of the C₁₄-C₁₈ dimer formation.

538 For C₁₉ dimers, due to the relatively smaller contribution of acyl RO₂ to C₉ and C₁₀ RO₂, their
539 ~~concentration-signal~~ decreases only by 10%-40%, and this reduction have contributions from both
540 acyl and alkyl RO₂. For C₂₀ dimers, their ~~concentration-signal~~ changes with the addition of NO₂ can
541 be discussed according to the number of hydrogen atoms in the molecules. Firstly, the ~~concentration~~
542 ~~signal~~ of C₂₀H₃₀O₇ and C₂₀H₃₀O₉ decreases by 40-60% with the addition of 30 ppb NO₂, indicating
543 a significant contribution of acyl RO₂ such as C₁₀H₁₅O₅-RO₂ (acyl RO₂ in default MCM v3.3.1) and
544 C₁₀H₁₅O₇-RO₂ in their formation, while other C₂₀H₃₀O_x dimers decrease by ~30%. The C₂₀H₃₂O_x
545 dimer series also exhibits a small reduction (less than 20%) with the addition of NO₂. However, the
546 C₂₀H₃₄O_x series shows an unexpected increase with the addition of NO₂ up to 10 ppb and almost
547 remains unchanged with the further increase of NO₂ concentration. Given that the cross-reaction
548 rate constant of acyl RO₂ can be orders of magnitude higher than that of counterpart alkyl RO₂
549 (Orlando and Tyndall 2012, Atkinson et al. 2007), the rapid consumption of acyl RO₂ by NO₂ would
550 preserve the alkyl RO₂ that tend to react with acyl RO₂ at a fast rate in the absence of NO₂, which
551 to some extent would elevate the concentration of alkyl RO₂ in the system and thus promote the less
552 competitive alkyl RO₂ + alkyl RO₂ reactions to form C₂₀H₃₄O_x dimers. The slight increase of some

553 $C_{10}H_{18}O_x$ -HOMs with the addition of NO_2 up to 10 ppb could also be due to this reason.

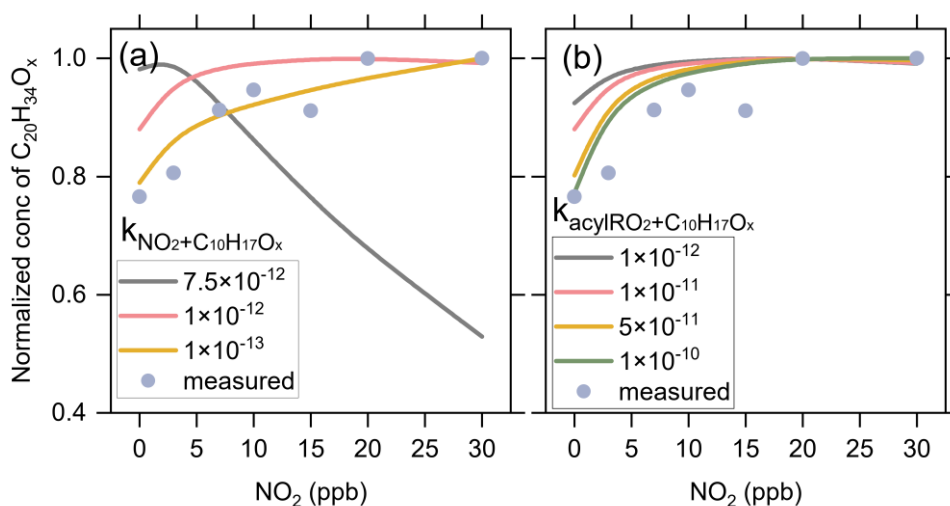


554
 555 Figure 10 Averaged normalized concentration-signal of the measured C_{14} - C_{20} dimers as a function
 556 of the added NO_2 concentration (Exps 1-28).

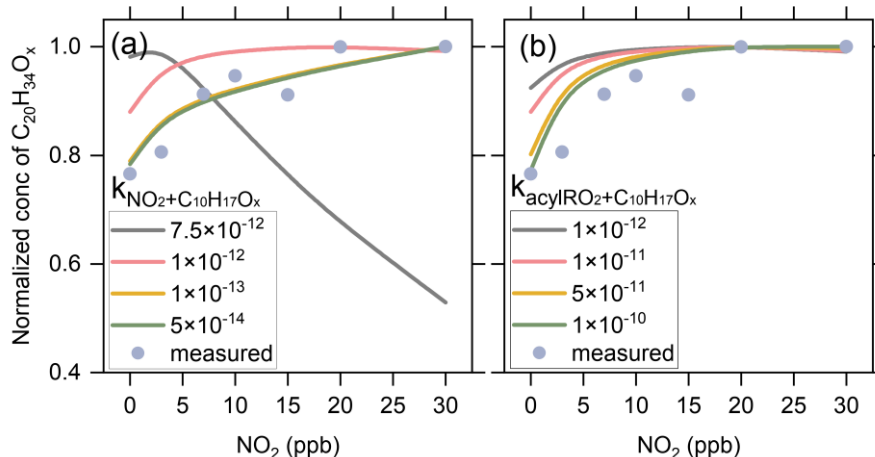
557 According to the noticeable increasing trend in $C_{20}H_{34}O_x$ as compared to other C_{20} dimers, we
 558 speculate that acyl RO_2 react faster with $C_{10}H_{17}O_x$ alkyl RO_2 than with $C_{10}H_{15}O_x$ alkyl RO_2 .
 559 Therefore, when the acyl RO_2 is depleted, the preservation of $C_{10}H_{17}O_x$ - RO_2 is more significant and
 560 the promotion of their cross-reactions to form $C_{20}H_{34}O_x$ is more evident. It is also possible that the
 561 reaction of NO_2 with $C_{10}H_{17}O_x$ alkyl RO_2 is less efficient compared to the reaction with $C_{10}H_{15}O_x$
 562 alkyl RO_2 , so more $C_{10}H_{17}O_x$ than $C_{10}H_{15}O_x$ are available for dimer formation in the presence of
 563 NO_2 .

564 To further prove the above two speculations, we performed sensitivity analyses for the reaction rates
 565 of $C_{10}H_{17}O_x$ - RO_2 using the F0AM model. Figures 11a show the changes in $C_{20}H_{34}O_x$ dimers with
 566 NO_2 addition at different $C_{10}H_{17}O_x$ - RO_2 + NO_2 reaction rates under the conditions of Exps 8-14. As
 567 the reaction rate varies from 5.1×10^{-14} to 1×10^{-12} cm^3 molecule $^{-1}$ s $^{-1}$, the increasing trend of

568 $C_{20}H_{34}O_x$ dimers versus the added NO_2 concentration is significantly weakened and the simulations
 569 are is more deviated from the measurements. When the reaction rate increases to $7.5 \times 10^{-12} \text{ cm}^3$
 570 $\text{molecule}^{-1} \text{ s}^{-1}$, the $C_{20}H_{34}O_x$ dimers decrease significantly with increasing NO_2 , which is in striking
 571 contrast to the measurements. Figure 11b presents the sensitivity analysis results for the cross-
 572 reaction rate constants of acyl $RO_2 + C_{10}H_{17}O_x-RO_2$. As this rate constant varies from 1×10^{-12} to 1
 573 $\times 10^{-10} \text{ cm}^3 \text{ molecule}^{-1} \text{ s}^{-1}$, the increasing trend of $C_{20}H_{34}O_x$ versus the NO_2 concentration is more
 574 pronounced and more consistent with the measurements. These sensitivity analyses support our
 575 speculation that the $C_{10}H_{17}O_x$ alkyl RO_2 may be different from other alkyl RO_2 radicals in terms of
 576 the reaction efficiency with NO_2 and acyl RO_2 species, which leads to different responses of
 577 $C_{20}H_{34}O_x$ dimers to NO_2 addition compared to other C_{20} dimers. These results also suggest that the
 578 presence of acyl RO_2 could affect the fate and contribution of alkyl RO_2 to HOM formation in
 579 atmospheric oxidation systems given the different reactivity of acyl RO_2 from alkyl RO_2 .



580



581

582 Figure 11 Sensitivity analyses of $C_{20}H_{34}O_x$ dimer production to (a) the reaction rates of NO_2 with
 583 $C_{10}H_{17}O_x-RO_2$ (a), and (b) the cross-reaction rate of acyl RO_2 with $C_{10}H_{17}O_x-RO_2$ (b), considering

584 a $C_{10}H_{17}O_x-RO_2 + NO_2$ reaction rate of 1×10^{-12} cm³ molecule⁻¹ s⁻¹ for $C_{10}H_{17}O_x-RO_2 + NO_2$.

585 4. Conclusions

586 In this study, the molecular identities, formation mechanisms, and contributions of acyl RO₂ to the
587 formation of HOMs during ozonolysis of α -pinene are investigated using a combination of flow
588 reactor experiments and detailed kinetic model simulations. Based on the marked decrease in RO₂
589 ~~concentration-signal~~ as a function of initial NO₂ concentration, a total of 10 acyl RO₂ are identified
590 during α -pinene ozonolysis. The acyl RO₂ contributes to 67%, 94% and 32% of C₇, C₈ and C₉ highly
591 oxygenated RO₂ but only 0.45% of C₁₀ highly oxygenated RO₂, respectively. Three main pathways
592 are identified for the formation of monoterpene-derived acyl RO₂: (i) the autoxidation of RO₂
593 containing aldehyde groups, (ii) the cleavage of C-C bond of RO containing an α -ketone group, and
594 (iii) the intramolecular H-shift of RO containing an aldehyde group. The autoxidation of aldehydic
595 RO₂ formed involving multiple RO decomposition or ring-opening steps plays a dominant role in
596 the formation of the highly oxygenated acyl RO₂ radicals (oxygen atom number ≥ 6), while the
597 less-oxygenated acyl RO₂ (oxygen atom number < 6) are mainly derived from the other two
598 pathways.

599 The acyl RO₂-involved reactions explain 50-90% of C₇ and C₈ HOM monomers and 14% of C₁₀
600 HOMs, respectively. For C₉ HOMs, this contribution can be up to 30%-60%. For the HOM dimers,
601 acyl RO₂-involved reactions contribute 50%-95% to the formation of C₁₄-C₁₈ dimers. Owing to the
602 higher cross-reaction rate constant of acyl RO₂ compared to alkyl RO₂, the acyl RO₂ + alkyl RO₂
603 reaction would outcompete the alkyl RO₂ + alkyl RO₂ reaction. Therefore, the rapid consumption
604 of acyl RO₂ by NO₂ in the experiments (as well as in polluted atmospheres) would make the alkyl
605 RO₂ that are supposed to react with acyl RO₂ retained, which to some extent elevates the
606 concentration of alkyl RO₂ in the system and thus promotes the reaction of alkyl RO₂ + alkyl RO₂
607 to form dimers such as C₂₀H₃₄O_x. The contribution of H-abstraction of α -pinene by OH radical to
608 the formation of acyl RO₂ and HOMs is found to be negligible in the absence of NO. This is because
609 the primary C₁₀H₁₅O₂-RO₂ radicals formed in such pathways are least-oxidized and thus have
610 relatively low cross-reaction efficiency to produce RO radicals, which are the key intermediates for
611 the formation of acyl RO₂ and HOMs in that channel. However, in the presence of NO, the formation
612 of highly oxygenated acyl RO₂ via the H-abstraction pathway is demonstrated, consistent with
613 previous studies (Shen et al., 2022).

614 In this study, acyl RO₂ species are identified according to a dramatic decrease in their ~~concentration~~
615 ~~signal~~ with the addition of NO₂. It should be noted that the presence of NO₂ could also inhibit the
616 formation of alkyl RO₂ species involving acyl RO₂ reactions. If there are any contributions of alkyl

617 RO₂ to acyl RO₂ identified in this study, the influence of such alkyl RO₂ species on HOM formation
618 would reflect an indirect effect of acyl RO₂. However, given that the formation of most of the acyl
619 RO₂ identified in this study can be reasonably explained by the proposed mechanisms and verified
620 by their responses to the addition of NO, the acyl RO₂ identified here are expected to have no
621 significant contributions from alkyl RO₂. Currently, the reaction kinetics of monoterpene-derived
622 acyl RO₂ are still poorly understood. Considering the important contribution of acyl RO₂ to HOM
623 formation, further kinetic studies are needed to get more specific rate constants for their autoxidation
624 and cross-reactions, thereby deepening our understanding of the role of acyl RO₂ in HOM and SOA
625 formation under atmospheric conditions.

626

627 *Data availability.* The data presented in this work are available upon request from the corresponding
628 author.

629

630 *Author contributions.* YZ and HZ designed the study, HZ, DH and JZ performed the experiments.
631 YZ and HZ analyzed the data, conducted model simulations, and wrote the paper. All other authors
632 contributed to discussion and writing.

633

634 *Competing interests.* The authors declare no conflict of interest.

635

636 *Acknowledgments.* Yue Zhao acknowledges the Program for Professor of Special
637 Appointment (Eastern Scholar) at Shanghai Institutions of Higher Learning.

638

639 *Financial support.* This work was supported by the National Natural Science Foundation
640 of China (grants 22022607, 21806104, and 42005090) and the Program for Professor of
641 Special Appointment (Eastern Scholar) at Shanghai Institutions of Higher Learning.

642

643 **References**

644 Atkinson, R., Hasegawa, D., and Aschmann, S. M.: Rate constants for the gas-phase reactions of O₃ with
645 a series of monoterpenes and related compounds at 296 ± 2 K, *Int. J. Chem. Kinet.*, 1221,
646 <https://doi.org/10.1002/kin.550220807>, 1990.

647 Atkinson, R., Baulch, D., Cox, R., Crowley, J., Hampson, R., Hynes, R., Jenkin, M., Rossi, M., and Troe,
648 J.: Evaluated kinetic and photochemical data for atmospheric chemistry: Volume III—gas phase
649 reactions of inorganic halogens, *Atmos. Chem. Phys.*, 7, 981-1191, [https://doi.org/10.5194/acp-7-](https://doi.org/10.5194/acp-7-981-2007)
650 981-2007, 2007.

651 Bell, D. M., Wu, C., Bertrand, A., Graham, E., Schoonbaert, J., Giannoukos, S., Baltensperger, U., Prevot,
652 A., Riipinen, I., and Haddad, I. E.: Particle-phase processing of α-pinene NO₃ secondary organic
653 aerosol in the dark, *Atmos. Chem. Phys.*, 13167–13182, [https://doi.org/10.5194/acp-22-13167-](https://doi.org/10.5194/acp-22-13167-2022)
654 2022, 2021.

655 Berndt, T.: Peroxy radical processes and product formation in the OH radical-initiated oxidation of alpha-

656 pinene for near-atmospheric conditions, *J. Phys. Chem. A*, 125, 9151-9160,
657 <https://doi.org/10.1021/acs.jpca.1c05576>, 2021.

658 Berndt, T.: Peroxy radical and product formation in the gas-phase ozonolysis of alpha-pinene under near-
659 atmospheric conditions: occurrence of an additional series of peroxy radicals O₂O-
660 C₁₀H₁₅O(O₂)_yO₂ with y = 1-3, *J. Phys. Chem. A*, 126, 6526-6537,
661 <https://doi.org/10.1021/acs.jpca.2c05094>, 2022.

662 Berndt, T., Mentler, B., Scholz, W., Fischer, L., Herrmann, H., Kulmala, M., and Hansel, A.: Accretion
663 product formation from ozonolysis and OH radical reaction of alpha-pinene: mechanistic insight
664 and the influence of isoprene and ethylene, *Environ. Sci. Technol.*, 52, 11069-11077,
665 <https://doi.org/10.1021/acs.est.8b02210>, 2018.

666 Berndt, T., Richters, S., Jokinen, T., Hyttinen, N., Kurtén, T., Otkjær, R. V., Kjaergaard, H. G., Stratmann,
667 F., Herrmann, H., and Sipilä, M.: Hydroxyl radical-induced formation of highly oxidized organic
668 compounds, *Nat. Commun.*, 7, 1-8, <https://doi.org/10.1038/ncomms13677>, 2016.

669 Bianchi, F., Kurtén, T., Riva, M., Mohr, C., Rissanen, M. P., Roldin, P., Berndt, T., Crouse, J. D.,
670 Wennberg, P. O., and Mentel, T. F.: Highly oxygenated organic molecules (HOM) from gas-phase
671 autoxidation involving peroxy radicals: A key contributor to atmospheric aerosol, *Chem. Rev.*, 119,
672 3472-3509, 2019.

673 Calvert, J. G., Derwent, R. G., Orlando, J. J., Wallington, T. J., and Tyndall, G. S.: Mechanisms of
674 atmospheric oxidation of the alkanes, 2008.

675 Claffin, M. S., Krechmer, J. E., Hu, W., Jimenez, J. L., and Ziemann, P. J.: Functional group composition
676 of secondary organic aerosol formed from ozonolysis of α -pinene under high VOC and autoxidation
677 conditions, *ACS Earth Space Chem.*, 2, 1196-1210,
678 <https://doi.org/10.1021/acsearthspacechem.8b00117>, 2018.

679 Ehn, M., Thornton, J. A., Kleist, E., Sipilä, M., Junninen, H., Pullinen, I., Springer, M., Rubach, F.,
680 Tillmann, R., and Lee, B.: A large source of low-volatility secondary organic aerosol, *Nature*, 506,
681 476-479, <https://doi.org/10.1038/nature13032>, 2014.

682 Fry, J., Kiendler-Scharr, A., Rollins, A., Wooldridge, P., Brown, S., Fuchs, H., Dubé, W., Mensah, A., Dal
683 Maso, M., and Tillmann, R.: Organic nitrate and secondary organic aerosol yield from NO₃
684 oxidation of β -pinene evaluated using a gas-phase kinetics/aerosol partitioning model, *Atmos.*
685 *Chem. Phys.*, 9, 1431-1449, <https://doi.org/10.5194/acp-9-1431-2009>, 2009.

686 Fry, J. L., Draper, D. C., Barsanti, K. C., Smith, J. N., Ortega, J., Winkler, P. M., Lawler, M. J., Brown,
687 S. S., Edwards, P. M., and Cohen, R. C.: Secondary organic aerosol formation and organic nitrate
688 yield from NO₃ oxidation of biogenic hydrocarbons, *Environ. Sci. Technol.*, 48, 11944-11953,
689 <https://doi.org/10.1021/es502204x>, 2014.

690 Guenther, A., Jiang, X., Heald, C. L., Sakulyanontvittaya, T., Duhl, T. a., Emmons, L., and Wang, X.:
691 The model of emissions of gases and aerosols from nature version 2.1 (MEGAN2. 1): an extended
692 and updated framework for modeling biogenic emissions, *Geosci. Model Dev.*, 5, 1471-1492,
693 <https://doi.org/10.5194/gmd-5-1471-2012>, 2012.

694 Iyer, S., Rissanen, M. P., Valiev, R., Barua, S., Krechmer, J. E., Thornton, J., Ehn, M., and Kurten, T.:
695 Molecular mechanism for rapid autoxidation in alpha-pinene ozonolysis, *Nat. Commun.*, 12, 878,
696 <https://doi.org/10.1038/s41467-021-21172-w>, 2021.

697 Jenkin, M., Young, J., and Rickard, A.: The MCM v3.3.1 degradation scheme for isoprene, *Atmos. Chem.*
698 *Phys.*, 15, 11433-11459, <https://doi.org/10.5194/acp-15-11433-2015>, 2015.

699 Jokinen, T., Sipilä, M., Richters, S., Kerminen, V. M., Paasonen, P., Stratmann, F., Worsnop, D., Kulmala,

700 M., Ehn, M., and Herrmann, H.: Rapid autoxidation forms highly oxidized RO₂ radicals in the
701 atmosphere, *Angew. Chem. Int. Ed.*, 53, 14596-14600, <https://doi.org/10.1002/anie.201408566>,
702 2014.

703 Junninen, H., Ehn, M., Petäjä, T., Luosujärvi, L., Kotiaho, T., Kostiainen, R., Rohner, U., Gonin, M.,
704 Fuhrer, K., and Kulmala, M.: A high-resolution mass spectrometer to measure atmospheric ion
705 composition, *Atmos. Meas. Tech.*, 3, 599-636, <https://doi.org/10.5194/amt-3-1039-2010>, 2010.

706 Kirchner, F., Thuener, L., Barnes, I., Becker, K., Donner, B., and Zabel, F.: Thermal lifetimes of
707 peroxy nitrates occurring in the atmospheric degradation of oxygenated fuel additives, *Environ. Sci.
708 Technol.*, 31, 1801-1804, <https://doi.org/10.1021/es9609415>, 1997.

709 [Knap, H. C. and Jørgensen, S.: Rapid Hydrogen Shift Reactions in Acyl Peroxy Radicals, *J. Phys. Chem.
710 A*, 121, 1470-1479, 10.1021/acs.jpca.6b12787, 2017.](#)

711 Knopf, D. A., Pöschl, U., and Shiraiwa, M.: Radial diffusion and penetration of gas molecules and aerosol
712 particles through laminar flow reactors, denuders, and sampling tubes, *Anal. Chem.*, 87, 3746-3754,
713 <https://doi.org/10.1021/ac5042395>, 2015.

714 Kristensen, K., Watne, Å. K., Hammes, J., Lutz, A., Petäjä, T., Hallquist, M., Bilde, M., and Glasius, M.:
715 High-molecular weight dimer esters are major products in aerosols from α -pinene ozonolysis and
716 the boreal forest, *Environ. Sci. Technol. Lett.*, 3, 280-285, 2016.

717 Kurten, T., Rissanen, M. P., Mackeprang, K., Thornton, J. A., Hyttinen, N., Jørgensen, S., Ehn, M., and
718 Kjaergaard, H. G.: Computational study of hydrogen shifts and ring-opening mechanisms in alpha-
719 pinene ozonolysis products, *J. Phys. Chem. A*, 119, 11366-11375,
720 <https://doi.org/10.1021/acs.jpca.5b08948>, 2015.

721 Li, X., Chee, S., Hao, J., Abbatt, J. P. D., Jiang, J., and Smith, J. N.: Relative humidity effect on the
722 formation of highly oxidized molecules and new particles during monoterpene oxidation, *Atmos.
723 Chem. Phys.*, 19, 1555-1570, <https://doi.org/10.5194/acp-19-1555-2019>, 2019.

724 Lin, C., Huang, R.-J., Duan, J., Zhong, H., and Xu, W.: Primary and secondary organic nitrate in
725 northwest China: a case study, *Environ. Sci. Technol. Lett.*, 8, 947-953,
726 <https://doi.org/10.1021/acs.estlett.1c00692>, 2021.

727 Meder, M., Peräkylä, O., Varelas, J. G., Luo, J., Cai, R., Zhang, Y., Kurtén, T., Riva, M., Rissanen, M.,
728 Geiger, F. M., Thomson, R. J., and Ehn, M.: Selective deuteration as a tool for resolving
729 autoxidation mechanisms in α -pinene ozonolysis, *Atmos. Chem. Phys.*, 23, 4373-4390,
730 <https://doi.org/10.5194/egusphere-2022-1131>, 2023.

731 Mentel, T., Springer, M., Ehn, M., Kleist, E., Pullinen, I., Kurtén, T., Rissanen, M., Wahner, A., and Wildt,
732 J.: Formation of highly oxidized multifunctional compounds: autoxidation of peroxy radicals
733 formed in the ozonolysis of alkenes—deduced from structure—product relationships, *Atmos. Chem.
734 Phys.*, 15, 6745-6765, <https://doi.org/10.5194/acp-15-6745-2015>, 2015.

735 Molteni, U., Simon, M., Heinritzi, M., Hoyle, C. R., Bernhammer, A.-K., Bianchi, F., Breitenlechner, M.,
736 Brilke, S., Dias, A., Duplissy, J., Frege, C., Gordon, H., Heyn, C., Jokinen, T., Kürten, A., Lehtipalo,
737 K., Makhmutov, V., Petäjä, T., Pieber, S. M., Praplan, A. P., Schobesberger, S., Steiner, G., Stozhkov,
738 Y., Tomé, A., Tröstl, J., Wagner, A. C., Wagner, R., Williamson, C., Yan, C., Baltensperger, U.,
739 Curtius, J., Donahue, N. M., Hansel, A., Kirkby, J., Kulmala, M., Worsnop, D. R., and Dommen, J.:
740 Formation of highly oxygenated organic molecules from α -pinene ozonolysis: chemical
741 characteristics, mechanism, and kinetic model development, *ACS Earth Space Chem.*, 3, 873-883,
742 <https://doi.org/10.1021/acsearthspacechem.9b00035>, 2019.

743 Noziere, B., Kalberer, M., Claeys, M., Allan, J., D'Anna, B., Decesari, S., Finessi, E., Glasius, M., Grgic,

744 I., and Hamilton, J. F.: The molecular identification of organic compounds in the atmosphere: state
745 of the art and challenges, *Chem. Rev.*, 115, 3919-3983, 2015.

746 Orlando, J. J. and Tyndall, G. S.: Laboratory studies of organic peroxy radical chemistry: an overview
747 with emphasis on recent issues of atmospheric significance, *Chem. Soc. Rev.*, 41, 6294-6317,
748 <https://doi.org/10.1039/C2CS35166H>, 2012.

749 Otkjær, R. V., Jakobsen, H. H., Tram, C. M., and Kjaergaard, H. G.: Calculated hydrogen shift rate
750 constants in substituted alkyl peroxy radicals, *J. Phys. Chem. A*, 122, 8665-8673,
751 <https://doi.org/10.1021/acs.jpca.8b06223>, 2018.

752 Pye, H., Chan, A., Barkley, M., and Seinfeld, J.: Global modeling of organic aerosol: the importance of
753 reactive nitrogen (NO_x and NO₃), *Atmos. Chem. Phys.*, 10, 11261-11276,
754 <https://doi.org/10.5194/acp-10-11261-2010>, 2010.

755 Roger, Atkinson, Sara, M., Aschmann, James, N., Pitts, and Jr.: Rate constants for the gas-phase reactions
756 of the OH radical with a series of monoterpenes at 294 ± 1 K, *Int. J. Chem. Kinet.*, 2004.

757 Shen, H., Vereecken, L., Kang, S., Pullinen, I., Fuchs, H., Zhao, D., and Mentel, T. F.: Unexpected
758 significance of a minor reaction pathway in daytime formation of biogenic highly oxygenated
759 organic compounds, *Sci. Adv.*, 8, eabp8702, <https://doi.org/10.1126/sciadv.abp8702>, 2022.

760 Sindelarova, K., Granier, C., Bouarar, I., Guenther, A., Tilmes, S., Stavrou, T., Müller, J.-F., Kuhn, U.,
761 Stefani, P., and Knorr, W.: Global data set of biogenic VOC emissions calculated by the MEGAN
762 model over the last 30 years, *Atmos. Chem. Phys.*, 14, 9317-9341, [https://doi.org/10.5194/acp-14-](https://doi.org/10.5194/acp-14-9317-2014)
763 [9317-2014](https://doi.org/10.5194/acp-14-9317-2014), 2014.

764 Tyndall, G., Cox, R., Granier, C., Lesclaux, R., Moortgat, G., Pilling, M., Ravishankara, A., and
765 Wallington, T.: Atmospheric chemistry of small organic peroxy radicals, *J. Geophys. Res.-Atmos.*,
766 106, 12157-12182, 2001.

767 Villenave, E. and Lesclaux, R.: Kinetics of the cross reactions of CH₃O₂ and C₂H₅O₂ radicals with
768 selected peroxy radicals, *J. Phys. Chem. C*, 100, 14372-14382, <https://doi.org/10.1021/jp960765m>,
769 1996.

770 Wang, Y., Zhao, Y., Li, Z., Li, C., Yan, N., and Xiao, H.: Importance of hydroxyl radical chemistry in
771 isoprene suppression of particle formation from α -pinene ozonolysis, *ACS Earth Space Chem.*, 5,
772 487-499, <https://doi.org/10.1021/acsearthspacechem.0c00294>, 2021.

773 Wolfe, G. M., Marvin, M. R., Roberts, S. J., Travis, K. R., and Liao, J.: The framework for 0-D
774 atmospheric modeling (F0AM) v3. 1, *Geosci. Model Dev.*, 9, 3309-3319,
775 <https://doi.org/10.5194/gmd-9-3309-2016>, 2016.

776 Xu, L., Møller, K. H., Crouse, J. D., Otkjær, R. V., Kjaergaard, H. G., and Wennberg, P. O.:
777 Unimolecular reactions of peroxy radicals formed in the oxidation of α -pinene and β -pinene by
778 hydroxyl radicals, *J. Phys. Chem. A*, 123, 1661-1674, <https://doi.org/10.1021/acs.jpca.8b11726>,
779 2019.

780 Yao, M., Zhao, Y., Hu, M., Huang, D., and Yan, N.: Multiphase reactions between secondary organic
781 aerosol and sulfur dioxide: kinetics and contributions to sulfate formation and aerosol aging,
782 *Environ. Sci. Technol. Lett.*, <https://doi.org/10.1021/acs.estlett.9b00657>, 2019.

783 Zhang, H., Yee, L. D., Lee, B. H., Curtis, M. P., Worton, D. R., Isaacman-VanWertz, G., Offenberg, J. H.,
784 Lewandowski, M., Kleindienst, T. E., and Beaver, M. R.: Monoterpenes are the largest source of
785 summertime organic aerosol in the southeastern United States, *Proc. Natl. Acad. Sci. U. S. A.*, 115,
786 2038-2043, <https://doi.org/10.1073/pnas.1717513115>, 2018.

787 Zhao, Y., Thornton, J. A., and Pye, H. O. T.: Quantitative constraints on autoxidation and dimer formation

788 from direct probing of monoterpene-derived peroxy radical chemistry, Proc. Natl. Acad. Sci. U. S.
789 A. , 115, 12142-12147, <https://doi.org/10.1073/pnas.1812147115>, 2018.

790 Zhao, Y., Yao, M., Wang, Y. Q., Li, Z. Y., Wang, S. Y., Li, C. X., and Xiao, H. Y.: Acylperoxy Radicals
791 as Key Intermediates in the Formation of Dimeric Compounds in alpha-Pinene Secondary Organic
792 Aerosol, Environ. Sci. Technol., 56, 14249-14261, 10.1021/acs.est.2c02090, 2022.

793 Zhao, Z. X., Zhang, W., Alexander, T., Zhang, X., Martin, D. B. C., and Zhang, H. F.: Isolating a-Pinene
794 Ozonolysis Pathways Reveals New Insights into Peroxy Radical Chemistry and Secondary Organic
795 Aerosol Formation, Environ. Sci. Technol., 55, 6700-6709, 10.1021/acs.est.1c02107, 2021.

796